Taylor & Francis
Taylor & Francis Group

Check for updates

Therapeutic strategies for Covid-19 based on molecular docking and dynamic studies to the ACE-2 receptors, Furin, and viral spike proteins

Essam S. A. E. H. Khattab (ID), Ahmed Ragab (ID), Mahmoud A. Abol-Ftouh (ID) and Ahmed A. Elhenawy (ID)

Department of Chemistry, Faculty of Science (Boys), Al-Azhar University, Nasr City, Cairo, Egypt

Communicated by Ramaswamy H. Sarma.

ABSTRACT

SARS-CoV-2 is a pandemic virus that caused infections and deaths in many world countries, including the Middle East. The virus-infected human cells by binding via ACE-2 receptor through the Spike protein of the virus with Furin's help causing cell membrane fusion leading to Covid-19-cell entry. No registered drugs or vaccines are triggering this pandemic viral disease yet. Our present work is based on molecular docking and dynamics simulation that performed to spike protein-ACE-2 interface complex, ACE-2 receptor, Spike protein (RBD), and Furin as targets for new small molecules. These drugs target new potential therapies to show their probabilities toward the active sites of mentioned proteins, strongly causing inhibition and/or potential therapy for covid-19. All target proteins were estimated against new target compounds under clinical trials and repurposing drugs currently present. Possibilities of those molecules and potential therapeutics acting on a certain target were predicted. MD simulations over 200 ns with molecular mechanics-generalized Born surface area (MMGBSA) binding energy calculations were performed. The structural and energetic analyses demonstrated the stability of the ligands-M^{Pros} complex. Our present work will introduce new visions of some biologically active molecules for further studies *in-vitro* and *in-vivo* for Covid-19, repurposing of these molecules should be taking place under clinical works and offering different strategies for drugs repurposing against Covid-19 diseases.

1. Introduction

The coronavirus disease, which was called Covid-19 by the WHO on February 11, 2020, began in Wuhan, China, in December 2019 and has highly spread in epidemic manners (Lillie et al., 2020). The international virus classification commission had clarified that the novel coronavirus was named SARS-CoV-2. COVID-19 is not the first virus combined with a severe respiratory disease caused by the coronavirus (Lai et al., 2020). However, in the past 20 years, coronaviruses have caused three epidemic diseases named SARS-Cov-2, SARS-Cov, and MERS-Cov (de Wit et al., 2016). Currently, cases of COVID-19 have been reported in many countries around the world, including Egypt (Wu et al., 2020). Coronaviruses are enveloped viruses with a positive-sense, single-stranded RNA genome (Su et al., 2016). Coronavirus Spike protein has been reported as a significant part of the virus-host cell entry (Papa et al., 2021). SARS-Cov-2, similar to SARS-Cov binds to human angiotensin-converting enzyme-2 (ACE2) through viral spike protein, which triggers the entry of infectious SARS-Cov-2 (Li et al., 2003; Zhou et al., 2020). A spike glycoprotein of SARS-CoV-2 (COVID-19) is a trimeric viral fusion protein that is existed S1 and S2 subunits that remain non-covalently presented in a nonbinding state (Hoffmann et al.,

2020; Tortorici & Veesler, 2019; Walls et al., 2020). Upon attachment of ACE2 by a receptor-binding domain (RBD) in the S1 subunit of spike protein (Wong et al., 2004), conformational rearrangements take place that causes S1 shedding and cleavage of the S2 subunit by host cell proteases, and exposure of a fusion peptide adjacent to the S2 proteolysis site (Madu et al., 2009; Millet & Whittaker, 2014; Tortorici & Veesler, 2019).

Angiotensin-converting enzyme-2 (ACE2) is a cardio-cerebral vascular protection factor found in many tissues, including the kidney, intestine, lung, skeletal muscles, and nervous system (Zahoor et al., 2021). Besides, it's played an important role in regulating blood pressure and anti-arteriosclerosis mechanisms (Miller & Arnold, 2019), as well as, it considers a major binding target for SARS-Cov-2 (Wrapp et al., 2020). SARS-CoV-2 differs from SARS-CoV by 380 amino acid sequencing, which translates to different five of the six crucial amino acids in the receptor-binding domain (RBD) that included in the S1 subunit between the viral spike (S) protein with cell membrane human ACE-2 (Durmaz et al., 2020). Spike protein of Covid-19 is studied to target therapeutic and vaccine development (Zhang et al., 2020). Otherwise, SARS-CoV-2 had found to use a wide variety of host

CONTACT Ahmed Ragab ✉ ahmed_ragab@azhar.edu.eg; ahmed_ragab7@ymail.com 🖅 Department of Chemistry, Faculty of Science (Boys), Al-Azhar University, Nasr City, Cairo 11884, Egypt; Mahmoud A. Abol-Ftouh ✉ biochemia770@yahoo.com 🖅 Department of Chemistry, Faculty of Science (Boys), Al-Azhar University, Nasr City, Cairo 11884, Egypt.

proteases including cathepsin L, cathepsin B, trypsin, factor X, elastase, Furin, and transmembrane protease serine 2 (TMPRSS2) for the S-protein that enhancing and facilitating cell entry following ACE-2 binding through the S2 subunit which reported as a membrane fusion unit (El-Shimy et al., 2021; Luan et al., 2020). Camostat mesylate is a serine protease inhibitor combined with a cathepsin L/B inhibitor blocked SARS-CoV-2 entry as it was trailing clinically in Japan (Millet & Whittaker, 2015).

In brief, the entry of both SARS-CoV and SARS-CoV-2 into cells is facilitated by the attachment of both RBD of viral spike protein and interfaced domains of the transmembrane ACE-2 proteins, followed by a cascade cell membrane fusion process result in virus-host cell entry (Yepes-Pérez et al., 2020). Besides, it had known that ACE-2 is a metalloenzyme and presents a zinc-binding active site (Chappel & Ferrario, 2006), since EDTA is a chelating agent of loosely bound Zn^{+2} metal ions, which acts as a cofactor for ACE-2 leading to Enzyme blocking (Wysocki et al., 2006).

On the other hand, it had reported that MLN-4760 is a specific inhibitor for ACE-2 in which their binding is irreversible (Shagufta & Ahmad, 2021). MLN-4760 has been used in numerous studies of ACE-2 inhibitor *in vivo* and *in vitro*. However, the compound is not currently commercially available, it has been shown to increase urinary albumin and mesangial cell expansion, vascular thickness in both type 1 and type 2 diabetic models (Soler et al., 2007; Ye et al., 2006). The entry of coronavirus is triggered by cleavage of Spike protein into two subunits as a subunit (S1) and (S2) by the action of proteolytic enzymes, including Furin proprotein (Yamada & Liu, 2009). Furin proprotein was found in most human tissues, including the small intestine, kidney, lungs, and liver, which explains why the viruses can invade different organs (Heald-Sargent & Gallagher, 2012).

The S1 subunit of Covid-19 binds to the ACE-2 receptor on the host cell membrane, while the S2 site interacts with the cell membrane to mediate receptor-dependent endocytosis (Yamada & Liu, 2009). The viral spike protein is essential for the entry of the virus into the cell, contains two functional domains: an ACE2 binding domain (also called receptor-binding domain-RBD), and a second domain essential for fusion of the viral and cell membranes through the action of Furin (Coutard et al., 2020; Walls et al., 2020; Wan et al., 2020). Furin activity reveals the binding and fusion domains, essential steps for entering the virus into the host cell (Zhao et al., 2020). Based on Furin's recognition substrate sequence characteristics, some short peptide inhibitors have been developed, such as Decanoyl-Arg-Val-Lys-Arg-chloromethyl ketone (DEC-RVKR-CMK) (Henrich et al., 2003; Matsuyama et al., 2018). DEC-RVKR-CMK is a small synthetic Furin inhibitor that is suitable for clinical purposes. Besides, it was used by many researchers as a reference inhibitor to study the effect of Furin and other proprotein convertases (Garten et al., 1994). It also strongly inhibits viral infection because of its ability to irreversibly block Furin (Becker et al., 2010). Furthermore, it had demonstrated that DEC-RVKR-CMK is a small irreversible cellular diffused competitive blocker of all proconvertases. Addition to it was reported to inhibit

fusion activity of viral glycoproteins and Furin-mediated cleavage and used as an antiviral agent, including duck hepatitis B virus (Tong et al., 2010), Chikungunya virus (Hallenberger et al., 1992), papillomavirus (Day & Schiller, 2009), chronic hepatitis B virus, influenza A, as well as Ebola virus infection (Ozden et al., 2008), and human immunodeficiency virus (Pang et al., 2013).

Currently, there are no registered drugs or vaccines available for beating Covid-19. SARS-CoV-2 is reported to be more infectious than other types of flu-viruses as one subject can infect more than two healthy subjects. Scientists are now giving intense attention to repurposing existing drugs. Researchers have suggested that using some of the registered antiviral drugs, e.g. HIV protease inhibitors and nucleoside analogs inhibitors, is a potential treatment method. Angiotensin-converting enzyme-2 (ACE-2) and RNA-dependent RNA polymerase (RdRp) are also promising therapeutics for COVID-19 infection (Shah et al., 2020). Some antiviral drugs clinically trialed against COVID-19 infection as Lopinavir, Favinapir, Ganciclovir, Oseltamivir, and Ritonavir as well as Hydroxychloroquine and Chloroquine, antimalarial drugs, has been proven to be effective in the treatments of COVID-19 (Devaux et al., 2020; Liu et al., 2020). Until any accurate treatment methodology is available for COVID- 19, using previously known either antiviral or other approved drugs that useful strategy. In the present work, molecular docking and molecular dynamics studies were performed over the binding pocket of COVID-19 and cell membrane receptors to show the potential effect of small compounds against coronavirus disease.

Based on the previous facts and our ongoing efforts to discover or develop a new heterocyclic compound with biological activity (Ammar et al., 2021; Ammar et al., 2020a;. Ammar et al., 2020b; El-Houseini et al., 2013; El-Sharief et al., 2019, 2016; Fayed et al., 2020; Hassan et al., 2020; Ragab et al., 2021; Rizk et al., 2020; Salem et al., 2020b; Wassel et al., 2021b, 2021a; Ammar et al., 2018; Ammar et al., 2016; Ammar et al., 2017). Our current study targets Furin to be an option for potential prevention of Sars-CoV-2 invading cell using DEC-RVKR-CMK as a Furin inhibitor where it had been used against HIV infection (Pang et al., 2013). Furthermore, the current study will estimate DEC-RVKR-CMK action on Covid 19, since, it was found that the Spike glycoprotein of Covid-19 has high similarity for HIV, ARAS-Cov and MERS-Cov (Pang et al., 2013; Van Lam van et al., 2019; Zhou et al., 2020). The previously mentioned researches pushed us to evaluate the potential therapeutic action of DEC-RVKR-CMK against Covid-19. Our study highlights the efficacy of DEC-RVKR-CMK as an interesting anti-Covid-19 agent through its binding ability. Additionally, this work aims to evaluate the ability of MLN-4760 and ethylene diamine tetra-acetate (EDTA) as inhibitors for ACE-2 (Vickers et al., 2002; Wysocki et al., 2006) by molecular modelling study, that may lead to interrupting the attachment of viral spike protein to the host cells. The computational docking and dynamics simulation studies will perform for viral spike protein, Furin, and spike-ACE-2 interface complex (Figure 1), encouraging more clinical trials using the previously mentioned drugs as potential
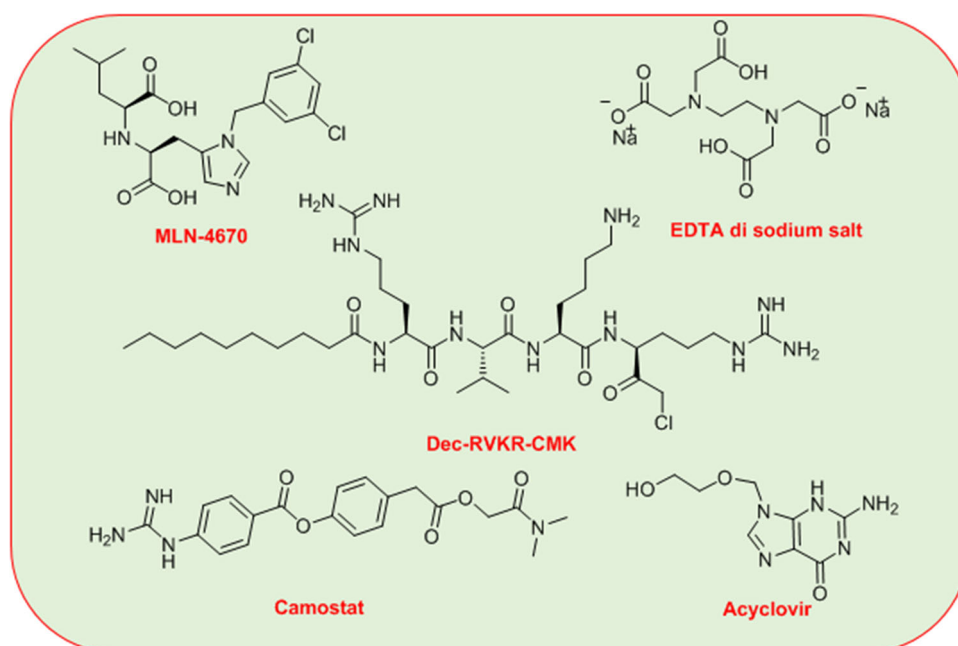
Figure 1. Structure of selected drugs with different biological targets.

elected therapeutics against SRAS-Cov-2 *in vitro* and *in vivo* studies.

2. Materials and methods

2.1. Ligand selection

The structure of selected drugs (MLN-4670 (Drug bank ID DB12271), Dec-RVKR-CMK (Pubchem ID 9962075), EDTA (Drug bank ID DB14600), Acyclovir (Drug bank ID DB00787) and Camostat (Drug bank ID DB13729), were obtained from a Drug bank (https://www.drugbank.ca/) and or sigma Merck (https://www.sigmaaldrich.com/european-export.html). The structures were introduced to gauss view, then fully optimized-geometries exported by density-functional theory (DFT) with B3LYP functional with STO-3G based set as implemented in Gaussian 09 package. The Open-Babel is used for generated sdf files.

2.2. Proteases M^Pro preparation

Crystal structure of the different protein as a structure of SARS-Cov-2 receptor-complexed with its human receptor ACE-2 'Spike-ACE-2 interface complex' (PDB ID: 6VW1). Structure of proprotein Furin as a ternary complex of proteinase K (PDB ID: 1PJ8) and native human angiotensin-converting enzyme-related carboxypeptidase ACE-2 (PDB ID: 1R42) were retractive from protein data bank (RCSB Protien Data Bank, 2020, https://www.rcsb.org/structure/6VW1, https://www.rcsb.org/structure/1p8j, and https://www.rcsb.org/structure/1R42). The protein structures were loaded separately. The protein structures were prepared by removing water, the polar H-atoms and electric charge were add using AMBER forcefield. Then M^Pros protonation state were tested using H^++server, and all missing hydrogen atoms were added (Gordon et al., 2005).

2.3. Molecular docking

Pre-molecular docking simulations were completed using Molecular Operating Environmental (MOE) software version 2008.10 (Hassan et al., 2021; Ibrahim et al., 2021a, 2021b). The docking processes for all drugs were performed according to the reported method (Fukuda et al., 2017) using the Triangle Matcher placement method and London dG as a scoring function. The top-scoring pose was inspected visually. The GlideSP module in Schrodinger was then applied for the final docking simulation steps (Sinha et al., 2020) (Supplementary materials).

2.4. Molecular dynamics (MD) simulation and molecular mechanics-generalized born solvent accessibility (MM-GBSA) analysis

MD simulations were parameterized with ANTECHAMBER using AMBER18. xLeap used for preparing the protein-ligand complexes to 200 ns MD simulations. Then, the 200 ns trajectories were applied to MM-GBSA analysis utilizing Amber18 tools on all the 5000 frames (Supplementary materials).

3. Results and discussion

3.1. Molecular docking study

The molecular docking study is one of the bioinformatics chemistry methods that widely used in the design of new drugs and active substances as well as decreasing the time and money spent on initial screening and identification of environmentally viable (Salem et al., 2020a). To reduce compactional-cost and time, we utilized two levels of molecular docking calculations. The pre-docking study by MOE and binding score were used for represented binding interaction and followed by a final docking level through glide score
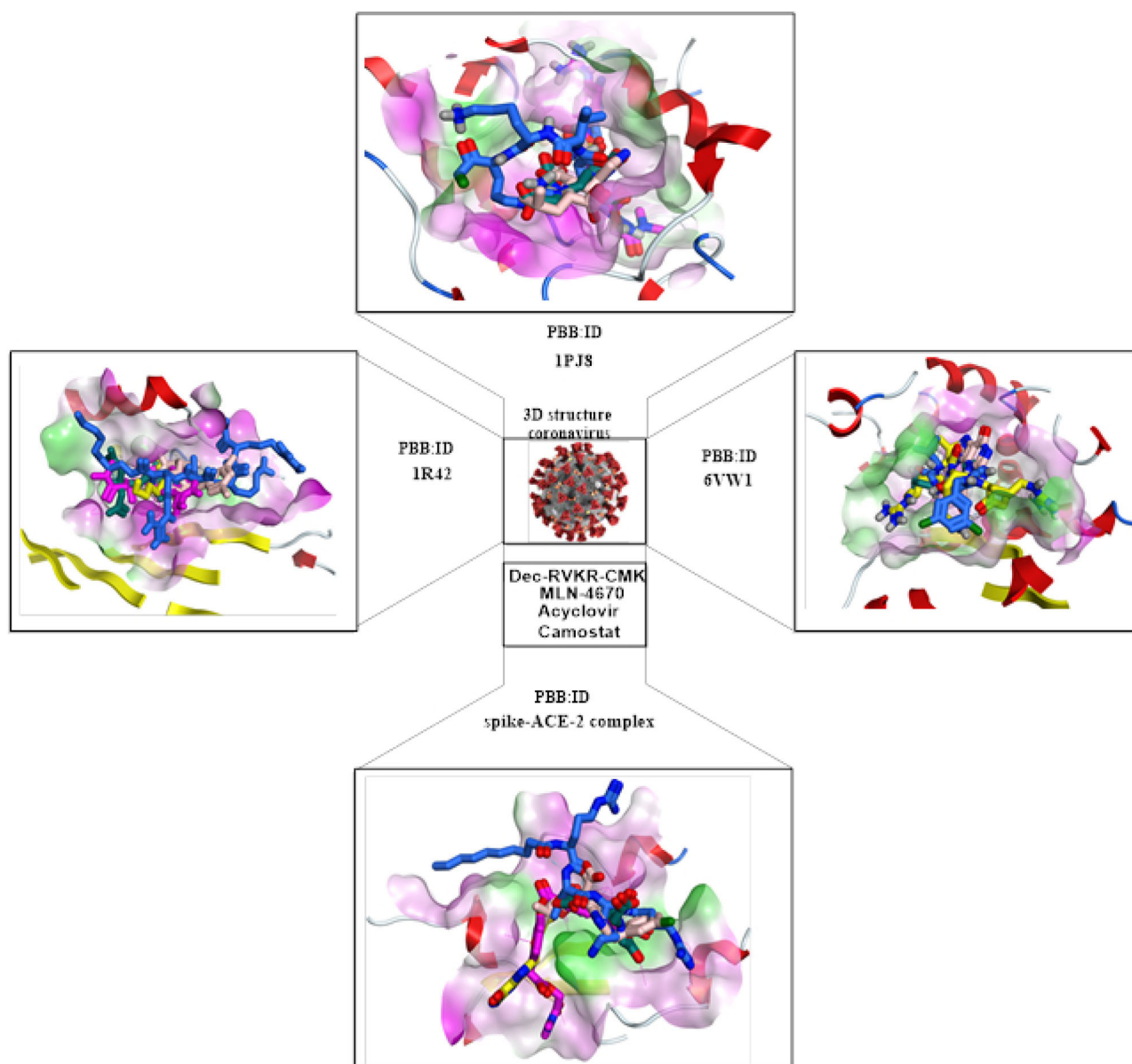
Figure 2. The GLID docking simulations for M^Pros and most stable investigated compounds after pre-docking by MOE; interactions were visualized using maestro tool; the investigated compounds were represented in the β-chain mode as; MLN-4670 as (Blue); Dec-RVKR-CMK (yellow); Acyclovir (red) and Camostat (light Orange).

(Figure 2), which is used for the further molecular dynamic study.

Our work strategy depending on the previous survey, suggested to use of five drugs that exhibited active biological values 'MLN-4670, Dec-RVKR-CMK, EDTA, Acyclovir and Camostat' were selected and docked inside different protein targets (Figure S1) to be used as a potential antiviral agent, especially against Covid-19, and among the numerous targets we focused on protein targets as Spike-ACE-2 interface complex, Spike protein, ACE-2 protein and Furin proprotein, and the results were represented in Table 1 (See supplementary information Table S1–S4 and all figures for MOE). Firstly, the viral spike protein-ACE-2 interface complex is the first step of SARS-Cov-2 infection where the Covid-19 binding to the human ACE-2, and therefore the virus entering the host cell leading to viral infection (Wong et al., 2004). The small molecules that had mentioned before were estimated as a

drug for docking inside active sites of Spike protein-ACE-2 interface complex (6VW1) (RCSB Protien Data Bank, 2020, https://www.rcsb.org/structure/6VW1, https://www.rcsb.org/structure/1p8j, and https://www.rcsb.org/structure/1R42). From Table 1, it observed that the pre-docking energy scores 'S' of drugs that attached to the host-virus complex, where is the highest 'S' was for EDTA disodium salt (-59.06 Kcal/mol) while for ACE-2 receptor (1R42) was (−10.59 Kcal/mol). It was observed that EDTA bind to the host-virus interface complex through the B chain of ACE-2 by two bonds, one sidechain hydrogen bond acceptor between Arg514 and the carbonyl group with bond length 2.68 Å. The second one is a backbone hydrogen bond acceptor between Ala 348 and oxygen of the same carboxylate with bond length 2.35 Å, as well as metalloenzyme Zn^{+2} formed one ionic bond with the oxygen of carboxylate (1.79 Å) and coordination bond with other carbonyl groups of EDTA (1.81 Å) inside the active site of the

Table 1. The Energy score (Kcal/mol) resulted from pre-docking by MOE and GLID docking of selected drugs inside the active site of targeted proteins.

	Target protein with PDB ID							
	Spike-ACE2 interface complex (6VW1)		Spike chain in ACE-2 complex (6VW1)		Furin Protein (1PJ8)		ACE-2 receptor (1R42)	
Drug Name	MOE	GLID	MOE	GLID	MOE	GLID	MOE	GLID
MLN-4670	−56.6 ± 2.54	−8.65	−19.54 ± 1.65	−9.63	−13.01 ± 1.42	−9.45	−16.91 ± 0.98	−5.524
Dec-RVKR-CMK	−41.64 ± 1.78	−7.36	−17.65 ± 1.35	−8.65	−26.49 ± 2.07	−9.76	−20.73 ± 1.32	−7.63
EDTA	−59.06 ± 3.25	−2.36	−8.78 ± 1.23	−2.45	−8.32 ± 0.51	−1.96	−10.59 ± 0.87	−1.09
Acyclovir	−23.09 ± 212	−8.56	−13.09 ± 1.59	−7.25	−17.60 ± 1.14	−7.86	−12.37 ± 1.03	−5.409
Camostat	−41.99 ± 2.84	−6.29	−20.78 ± 2.12	−7.48	−17.37 ± 0.97	−6.524	−18.94 ± 1.41	−5.87

Spike-ACE-2 interface complex. While docking of EDTA inside the active site of ACE-2 receptor (1R42) (RCSB Protien Data Bank, 2020, https://www.rcsb.org/structure/6VW1, https://www.rcsb.org/structure/1p8j, and https://www.rcsb.org/structure/1R42) showed only one sidechain donor between Asp206 and nitrogen of ethylenediamine with bond length 2.41 Å and Zn^{+2} ion not formed any bonds with EDTA drug although Zn^{+2} ions present in an active site (Figure 3, S1 & S2). Previously, EDTA disodium is used as a chelation therapy in many diseases such as atherosclerotic disease, angina (Grier & Meyers, 1993; Halbert, 2004; Lamas et al., 2013) and neurotoxicity (Fulgenzi & Ferrero, 2019) also EDTA is considered as ACE-2 inhibitor (Wysocki et al., 2006) since, it had demonstrated that an ACE-2 is a metalloenzyme containing Zn^{+2} binding active site (Chappel & Ferrario, 2006).

The final glide score for EDTA showed the lowest binding energy against all M^{Pros} so we determine stop further MD study for EDTA (Table 1). Furthermore, MLN-4670 is reported as a specific ACE-2 irreversible inhibitor (Vickers et al., 2002). The molecular docking simulation was performed for spike-ACE-2 interface complex inside the active site of (6VW1) and showed (BE) binding energy (S) = (−56.60 Kcal/mol) and by the same way, for only ACE-2 receptor (1R42), it was found energy score (S) = (−16.91 Kcal/mol) (Table 1). Its ligand showed the highest BEs in the final step of docking in the range (−9.63 to −5.524 Kcal/mol) against all M^{Pros} except Furin Protein (1PJ8).

The previously mentioned results observed that the binding of MLN-4670 is stronger when attached to the ACE-2 chain associated with the viral spike protein chain (6VW1) than binding separated ACE-2 receptors. The high binding energy of MLN-4670 inside the active site of (6VW1) may be due to the two ionic bonds between metalloenzyme Zn^{+2} and two oxygen atoms of carboxylate with bond length 1.77 and 1.75 Å, besides, hydrogen bond backbone acceptor between Ala 348 and carbonyl of carboxylate with bond length 2.53 Å (Figure S1 and S2). MLN-4670 showed the following bonds in the final step: two H-bonds between ALA348 as donor and carbonyl group, two π-π bonds between phenyl ring and TRP349, the hydrogen bond between Cl atom and ASP350, four ionic bonds between Zn and carbonyl groups, respectively (Figure S3). While in the case of redocking the MLN-4670 inside the receptor of the cell on (1R42) and reveled in both docking steps (Figure 3, S1 and S6), H-bond sidechain donor between Asp266 and nitrogen of secondary amine with bond length 2.34 Å and formed an ionic bond between Lys562 and carbonyl groups. Herein, we could highlight that the MLN-4670 are more effective against Covid-19 infection and practical works

needed for those drugs. Particularly, it has been observed that the docking study of the Spike protein-ACE-2 interface complex showed all bindings to the B chain that belonged to ACE-2 in the complex. So, we isolated the spike protein (E and F chains) from the complex based on a computational method to determine if it competes for the combining of drugs with ACE-2 chains. The MLN-4670 drug's affinity displayed binding energy S = (−19.54 and −9.63 Kcal/mol) respectively, for both steps. This ligand caped over Trp436 by carbonyl of carbonate with bond length 2.59 Å and Asn343 with NH group 2.84 Å, respectively. While, in the final step, MLN-4670 occupied the binding site by carboxylate group and amino group to formed H-bond and two ionic bonds between Arg490 and Glu271, respectively (Figure S4). The previously mentioned results observed that the spike protein could enhance the binding of drugs to the ACE-2 (A, B chains) in a complex, in addition to it is a competitive active binding site to spike only if all ACE-2 receptor sites is binding (Figures S1 and S2).

Furin is a proconvertase enzyme, and it is essential for the entry of SARS-Cov-2 into the host cells through its binding and fusion functional domains (Zhao et al., 2020). The blocking of Furin may inhibit the viral host cell entry (Baron et al., 2020; Kong et al., 2020). The docking study was achieved for Furin protein (1PJ8) (RCSB Protien Data Bank, 2020, https://www.rcsb.org/structure/6VW1, https://www.rcsb.org/structure/1p8j, and https://www.rcsb.org/structure/1R42), and the interaction of small molecules inside its active site represented in (Table 1). The results showed that DEC-RVKR-CMK was demonstrated as a Furin inhibitor (Pang et al., 2013). The DEC-RVKR-CMK showed the highest potent binding inhibitors for Furin among the studied molecules by showing the BE = (−26.49 and −9.76 Kcal/mol) when compared with both Camostat (S = −17.37 and −6.52 Kcal/mol) and Acyclovir (S = −17.60 and −7.86 Kcal/mol), respectively, for both steps. The DEC-RVKR-CMK formed three hydrogen bonds inside the active site of (1PJ8), two of three hydrogen bond sidechain donors through Asp 530 and nitrogen of imino (C=N) and nitrogen of NH of guanidine with bond length 2.72 and 2.30 Å, respectively. The third one is hydrogen bond backbone donor between Val263 and nitrogen of butylamine 2.46 Å (23%) as well as hydrophobic interaction due to aliphatic chains in the structure (Figures S1, S3 and S6). The final H-bond formed only in glide docking between carboxylate and Gly265 (Figure S6, Supplementary information S3).

Camostat mesylate is a serine protease inhibitor which a part of a proprotein facilitating SARS-CoV-2 entry, and it was trialing in Japan (Millet & Whittaker, 2015). It was first described in the literature in 1981, as part of research on the
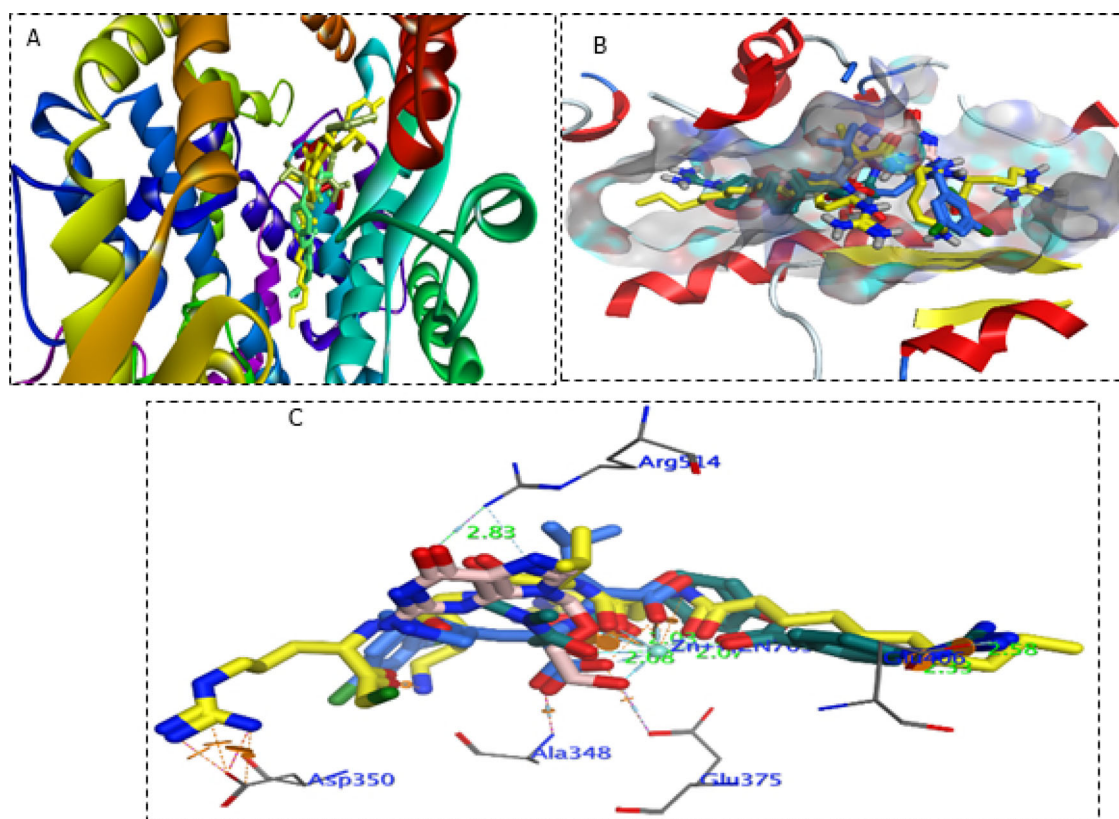
Figure 3. Interaction analysis for tested compounds against the SARS-CoV-2 viral Spike-ACE2 interface Complex (6VW1) during the MDs; (**A**) Equilibrated of tested compounds structure bound to the SARS-CoV-2 viral spike receptor-binding domain before MDS production phase; (**B**) Receptor surface analysis; (**C**) Ligand analysis; all tested ligands represented in stick mode; where DEC-RVKR-CMK (yellow); of Camostat (green); Acyclovir (orange); MLN-4670 (blue).

inhibition of skin tumors in mice (Ohkoshi, 1981). Camostat mesylate inhibits cholecystokinin, pro-inflammatory cytokines, and serine proteases, therefore, it had repurposing for treatment of Covid-19 (Hoffmann et al., 2020; Uno, 2020). Camostat mode of action was similar to a great extent with DEC-RVKR-CMK; otherwise, the DEC-RVKR-CMK showed higher interaction with Furin than Camostat. On the other hand, Acyclovir showed a near energy score binding to Camostat. Acyclovir was registered as a nucleotide analogue antiviral used to treat herpes simplex, *Varicella zoster*, herpes zoster, herpes labialis, and acute herpetic keratitis (Perry & Wagstaff, 1995; Sadjadi et al., 2018). We reused Acyclovir in the current molecular docking study to show its binding to the target's proteins. According to the current docking study, we compared the binding score of both Camostat and Acyclovir and showed no significant differences and clinical trials for Acyclovir are recommended as well as Camostat. On the other hand, DEC-RVKR-CMK showed the highest binding score to be the most interested in pushing more efforts with further research works (Figure 4**)**.

Furthermore, DEC-RVKR-CMK and Camostat showed nearly similar binding interactions against 1R42 and 6VW1 in both stages. The DEC-RVKR-CMK was demonstrated two hydrogen bonds sidechain donors between Asp350 and nitrogen of an imino (C $=$ NH) guanidine and nitrogen of the amino (NH$_2$) guanidine with bond length 2.40°A and 2.29°A. Moreover, two arene-cation interaction between Trp349 with the amino group of pentenyl amine derivative and His346 with the amino of guanidine moiety as well as Zn^{+2} ion form two coordinate

bonds with the carbonyl group with bond length 2.00°A, 1.95°A (Figure S1–S4 and S6). Similarly, Camostat showed two hydrogen bonds sidechain donors between Glu406 and the nitrogen of the imino (C $=$ NH) guanidine and nitrogen of an amino (NH) guanidine with bond length 2.58 and 2.33°A. Besides, one arene-arene-interaction with phenyl of the 4-guanidine benzoic acid derivative and Zn^{+2} ion form three coordinated bonds with three carbonyl groups with bond length ranged between 2.03 and 2.08°A for the Spike protein-ACE-2 interface complex. Simultaneously, both DEC-RVKR-CMK and Camostat were bound to Spike chains (E and F) separated from host-virus interface complex with binding energy S$=$ -17.65, -20.78 Kcal/mol, respectively. (supplementary material Table S1 and S2)

Finally, the present docking study hypothesized that the drugs used in our research interacted with more than one targeted proteins with high interaction docking BE means that using of one or more small molecules can block the binding site of SARS-CoV-2 with irreversible interactions and give high effect on infected cells with covid-19 practically. For example, using MLN-4670 and DEC-RVKR-CMK as potential therapies in a deep study, with respect to their dose's effects on healthy tissues and cells, may raise the possibility to prevent viral host cell entry and also may cure the infected cells with SARS-Cov-2. MLN-4670 showed the highest BE interaction for the Spike-ACE-2 complex and ACE-2 receptor, which is the mirror of free cells hoping to block cell receptors 'the Covid-19 site binding'. Another significant finding from BE, DEC-RVKR-CMK can bind Furin protein's active site with high supporting the prevention of virus-cell entry through inhibiting cell membrane fusion. All
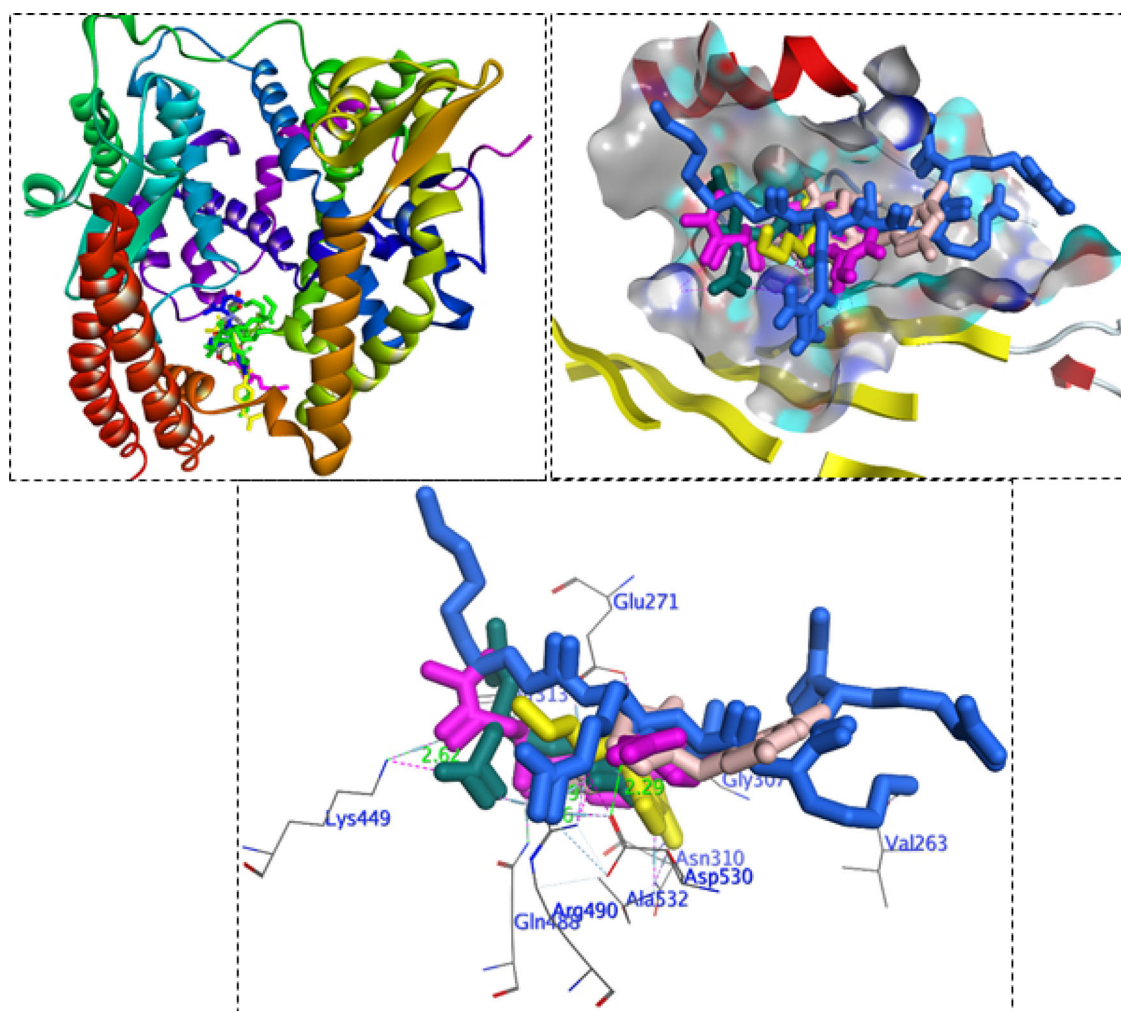
Figure 4. Interaction analysis for tested compounds against the SARS-CoV-2 viral **Furin Protein (1PJ8)** during the MDs; (A) Equilibrated of tested compounds structure bound to the SARS-CoV-2 viral spike receptor-binding domain before MDS production phase; (B) Receptor surface analysis; (C) Ligand analysis; all tested ligands represented in stick mode; where DEC-RVKR-CMK(yellow); of Camostat (green); Acyclovir (orange); MLN-4670 (blue).

the previous results that discussed and our conclusion depending on docking affinity binding energy that showed a high binding score addition to many other factors that support our work as the drugs selected already registered and approved for using as drugs on the market to another targeted diseases and that decrease spent time for designing a new drug that consumed time and money due to further experimental as well as, length and type of bonds in docking process were all bindings not exceeded than 3.25°A with a good strength percentage. Several hydrogen bonds and some other interactions appear as arene-arene or arene-cation interaction, and in some cases that protein-containing metalloenzyme Zn + 2 another type of bonds as coordination and ionic bonds appear with small bond length. According to the previous motioned strategies, it is vital to run out *in-vivo* and *in-vitro* studies to evaluate the effects of previously used drugs that could stop coronavirus's breakout (Covid 19).

3.2. MD simulations

To determine the reliability and stability of the binding affinity between drug and receptor, the MD-calculations (MDs) were performed according to this workflow, docking studies,

MDs and Free binding energy (BEs) calculation. MD was used to obtain dynamic data at spatial and picosecond (Benson & Daggett, 2012; Gajula et al., 2016). MDs have been performed in three phases of minimization. The first step is heating step and two equilibrium phases and consequently by 200 ns of the generation phase. The binding-mode of generated complexes was analyzed based on H-bond, *Van-der-Waals* and π-π interactions. The trajectories-MDs are analyzed through these parameters; RMSD and free 'BEs' binding energies/ Poisson-Boltzmann surface area (MM-PBSA), Radius-gyration (Rg), and SASA (solvent accessible surface area). The four M^{Pros} bind with four ligands showed stable and constant RMSD variation range 0.10 to 0.24 nm at on 200 ns timescale (Figure 5). Pre-MDs analysis for MLN-4670-complexes displays the conformational stability at 5 ns (RMSD = 1.5 nm) for all M^{Pros} except (6vwl) the stability appeared at 20 ns with RMSD= 1.46 nm. The stability for other complexes from post-MDs analysis appeared at 5 ns with RMSD range 1.46 to 1.49 nm (Figure 5).

For MLN-4670 against 6VW1 represented four different fluctuations at 5–15, 20–50, 108–120 and 162–184 ns against (RMSD) nm, this related to the conformational stability stages. The large fluctuation may be the change in the
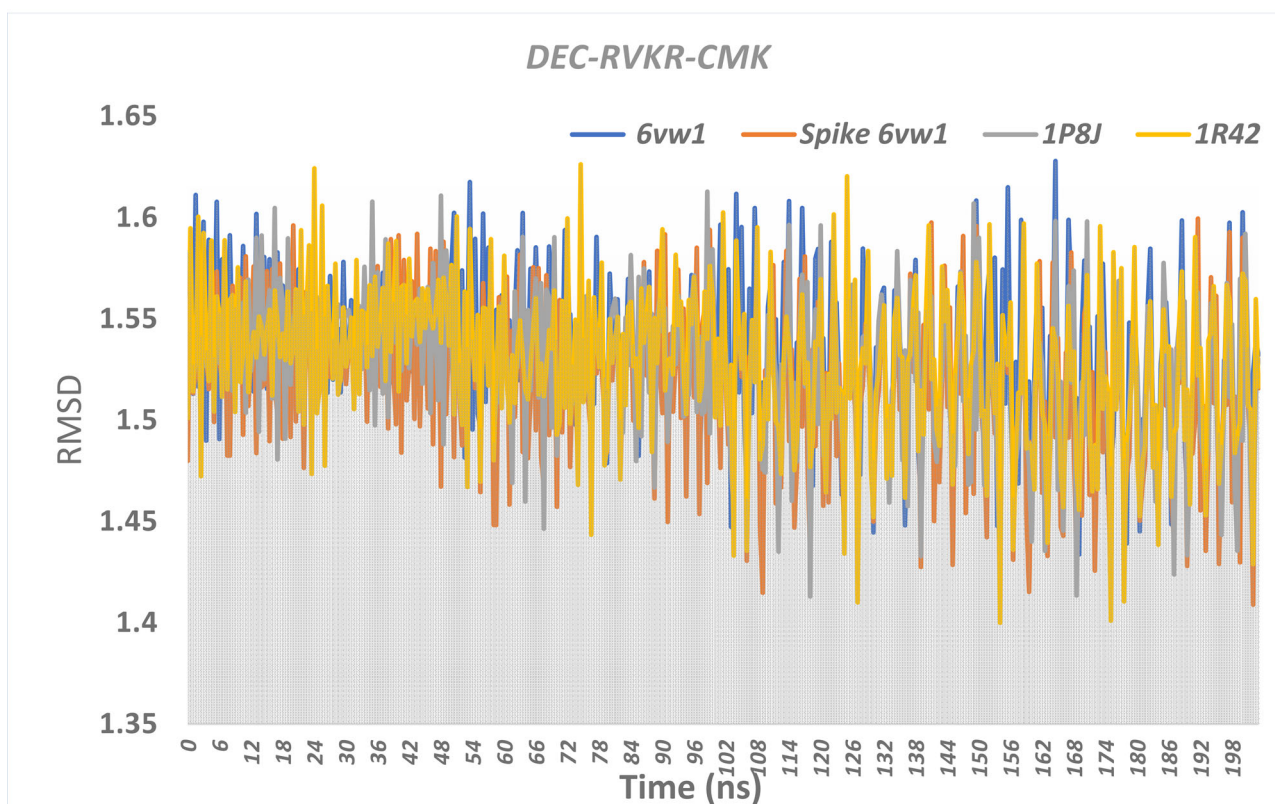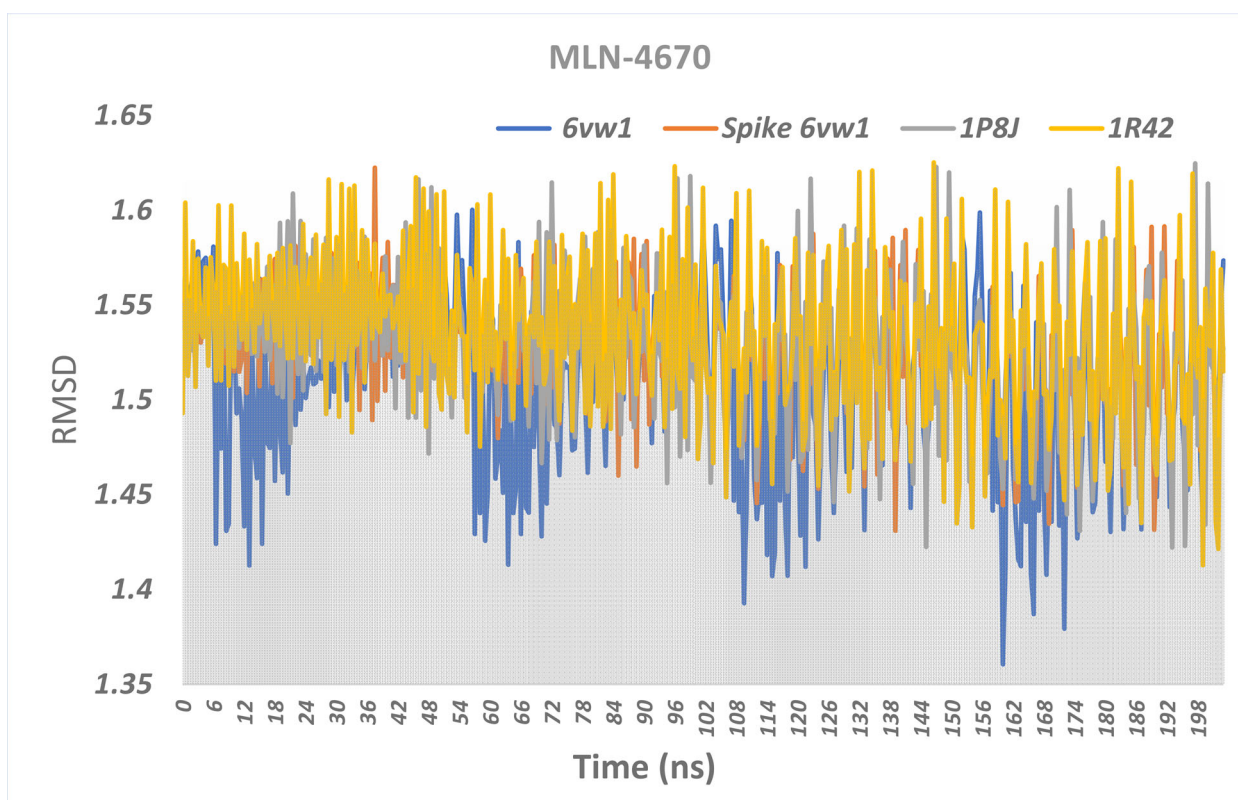
Figure 5. The RMSD analysis for ligands and M^{Pros} complexes; 6vwl-Complexes (Blue), spike 6vwl-Complexes (Red), 1P8J-Complexes (gray) and 1R42-Complexe (yellow).

conformation in the M^{Pros} binding-site. The large fluctuation appeared between 8–15 ns with RMSD > 1.44–1.55 nm. The other M^{Pros}-binding sites against MLN-4670 showed one stable conformational stage at all period-scales 5–200 ns. All M^{Pros}-binding sites of the protein structures are not affected.

For Dec-RVKR-CMK-M$^{Pros.}$, Camostat-M^{Pros} and Acyclovir-M^{Pros} figured stable RMSD with slight fluctuation for all M$^{Pros.}$ RMSD is constant and consistently fluctuated till end simulations at 200 ns period. Its compounds did not impact the backbone of protein-fluctuation and showed that the
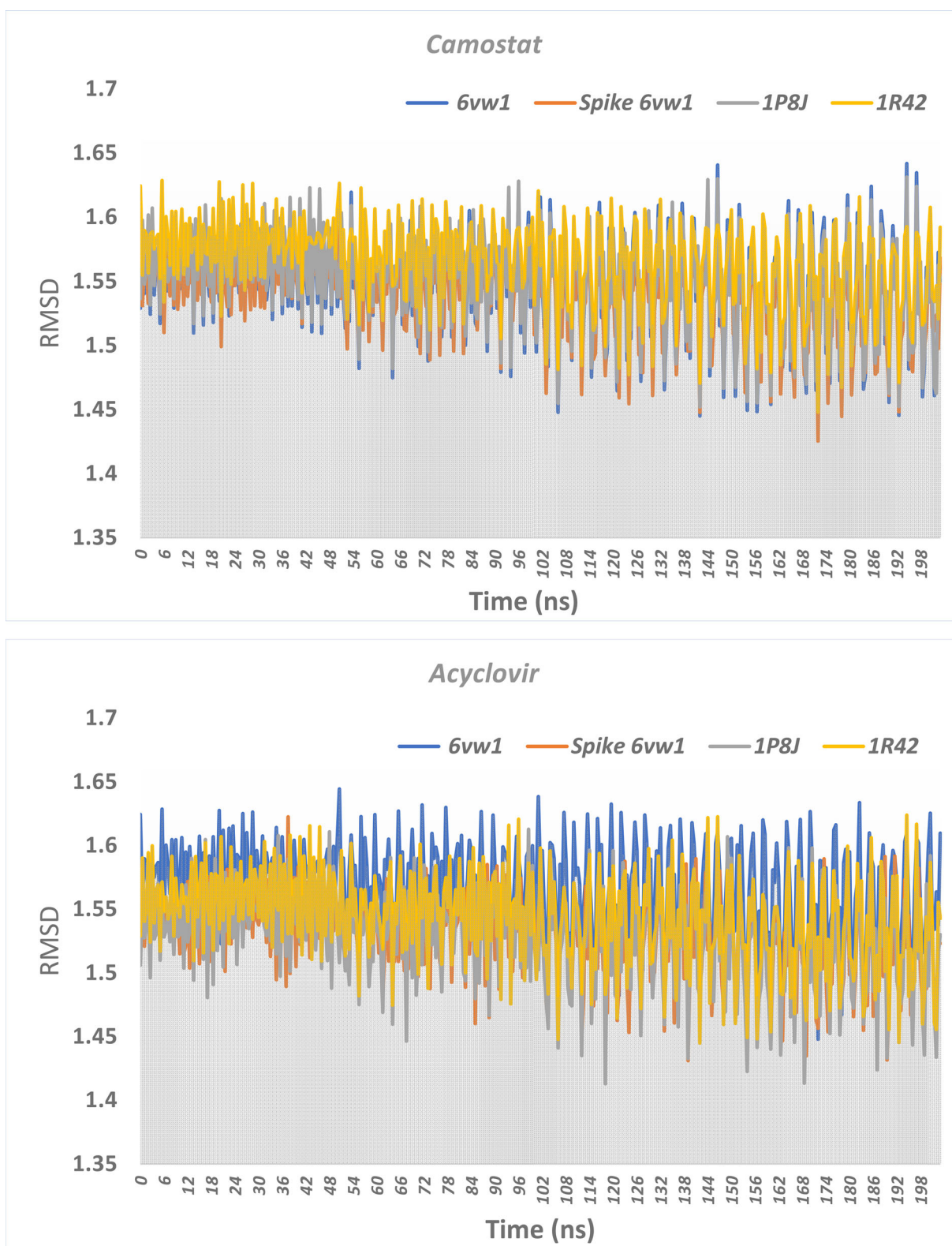
Figure 5. (Continued)

binding-site-proteins have fluctuations causing compounds-fluctuations during the computation process. It may explain by increasing binding-zone and the existence of a loop at this binding-zone.

3.3. Analysis of free BE/Poisson-Boltzmann surface area (MM-PBSA)

The pre-molecular docking proposed the binding energy (BE) of the complex. The ΔG or post docking process term
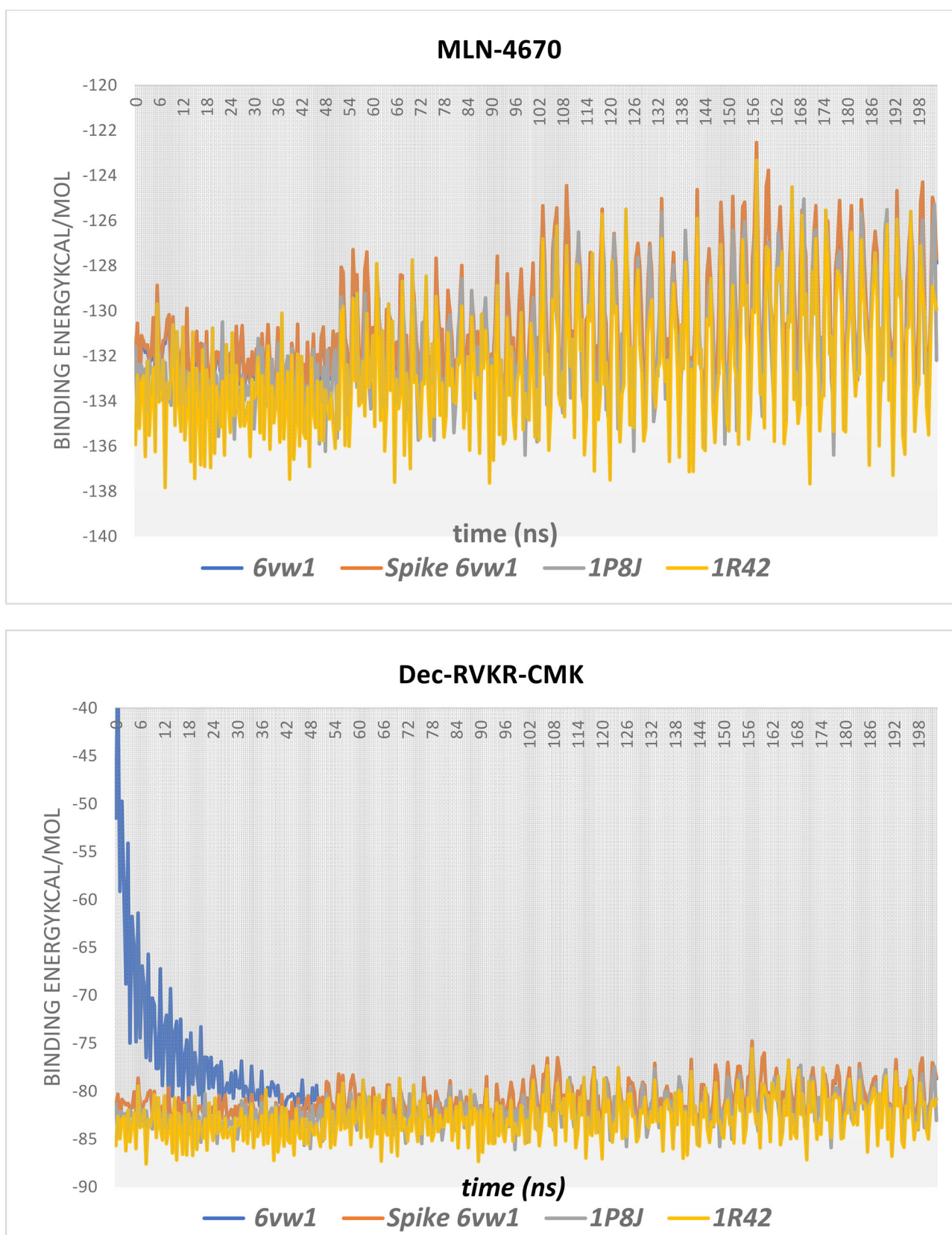
Figure 6. Calculated MM-GBSA binding energies over 200 ns for M^Pro complexes, 6vwl-Complexes (Blue), spike 6vwl-Complexes (Red), 1P8J-Complexes (gray) and 1R42-Complexe (yellow).
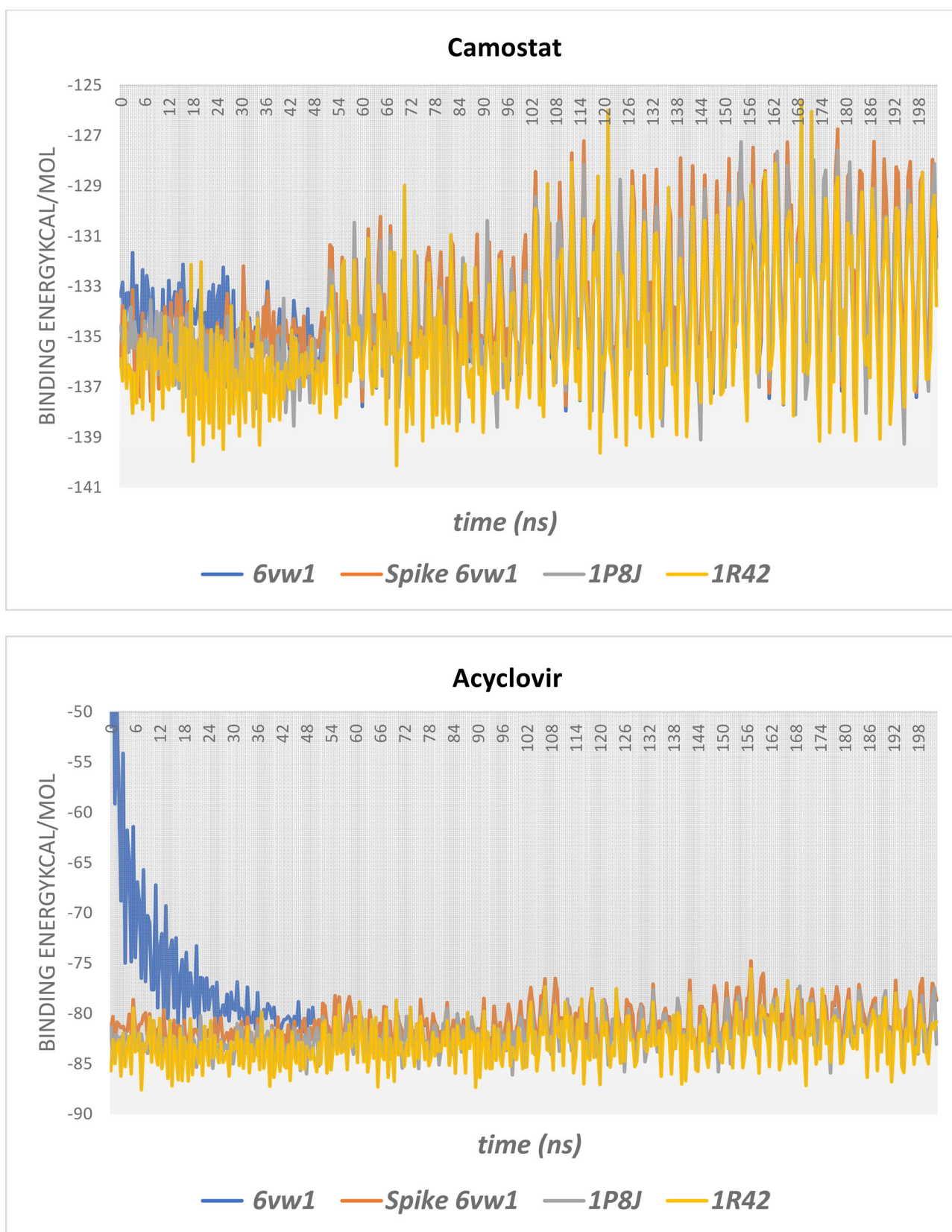
Figure 6. (Continued)

referred to the analysis of free BE after the simulation process, which examined the stability of non-bonding interactions between binding-site and compound. To get the high reliability degree, MD simulations for the docked-poses were achieved in a solvent along 200 ns, and the corresponding BEs were simulated by MM-GBSA basis set (Figure 6). All tested ligands exhibited high stability against MD simulations with promising MM-GBSA in range −40 to −140 kcal/mol.
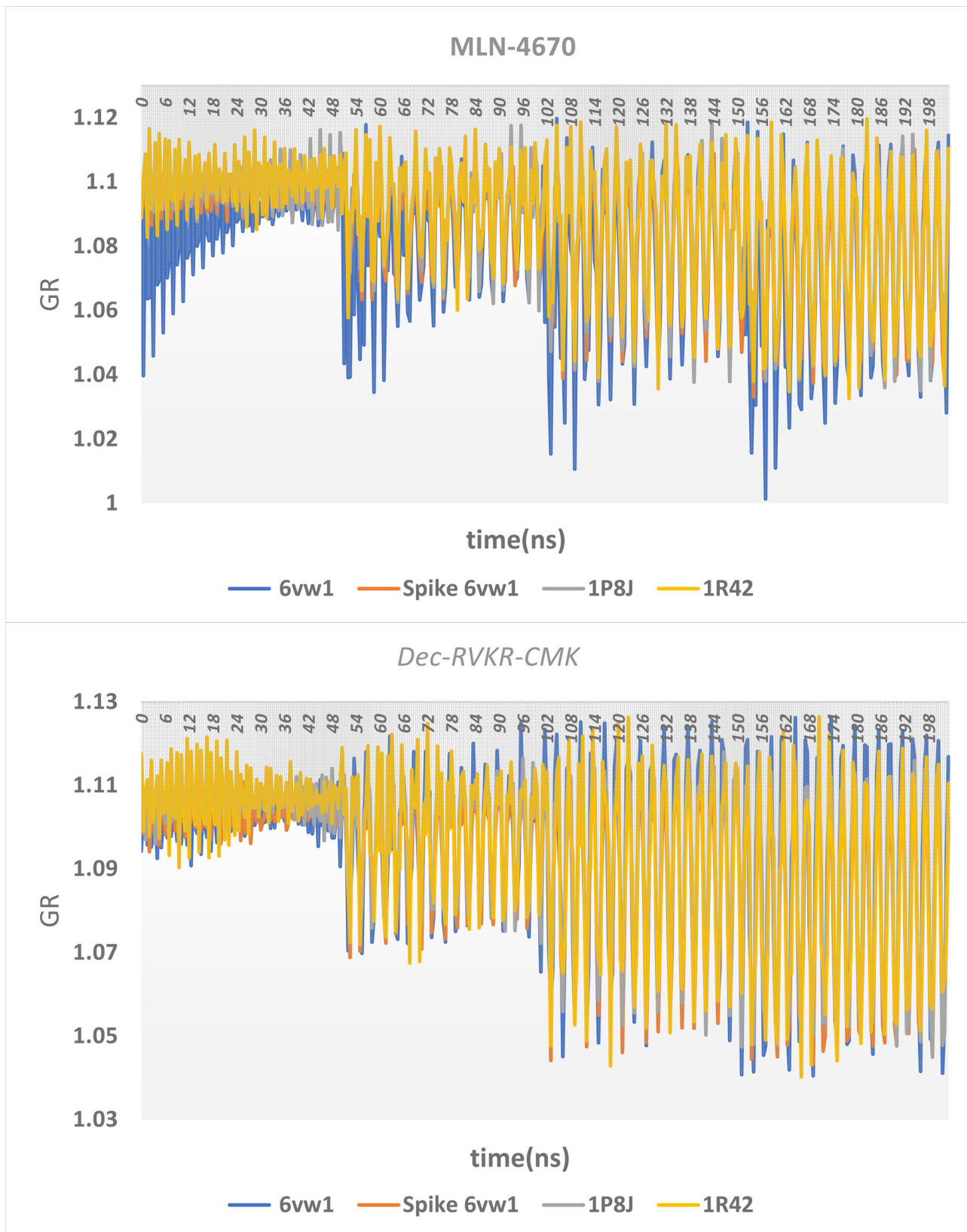
Figure 7. Radius of gyration (Rg) analysis for 6vwl-Complexes (Blue), spike 6vwl-Complexes (Red), 1P8J-Complexes (gray) and 1R42-Complexe (yellow).

For MLN-4670-M$^{Pros.}$ showed no significant oscillation for all M^{Pro}. In case of 6vwl complexed with *Dec-RVR-CMK* showed lower MM-GBSA (−40 to −80 kcal/mol) over 0–50 ns period. Its complex displayed no significant difference with enhancement values for MM-GBSA BEs over 20–200 ns. In

Acyclovir-6vwl (M^{Pro}), which showed lower binding affinity over 0–20 ns corresponding to MM-GBSA (−50 to −78 Kcal/mole). According to MM-GBSA BEs for all tested complexes, ligands' binding affinity is arranged as Dec-RVKR-CMK-M^{Pro} < Acyclovir-M^{Pro} < MLN-4670-M^{Pro} < Camostat-M^{Pro}. The slight
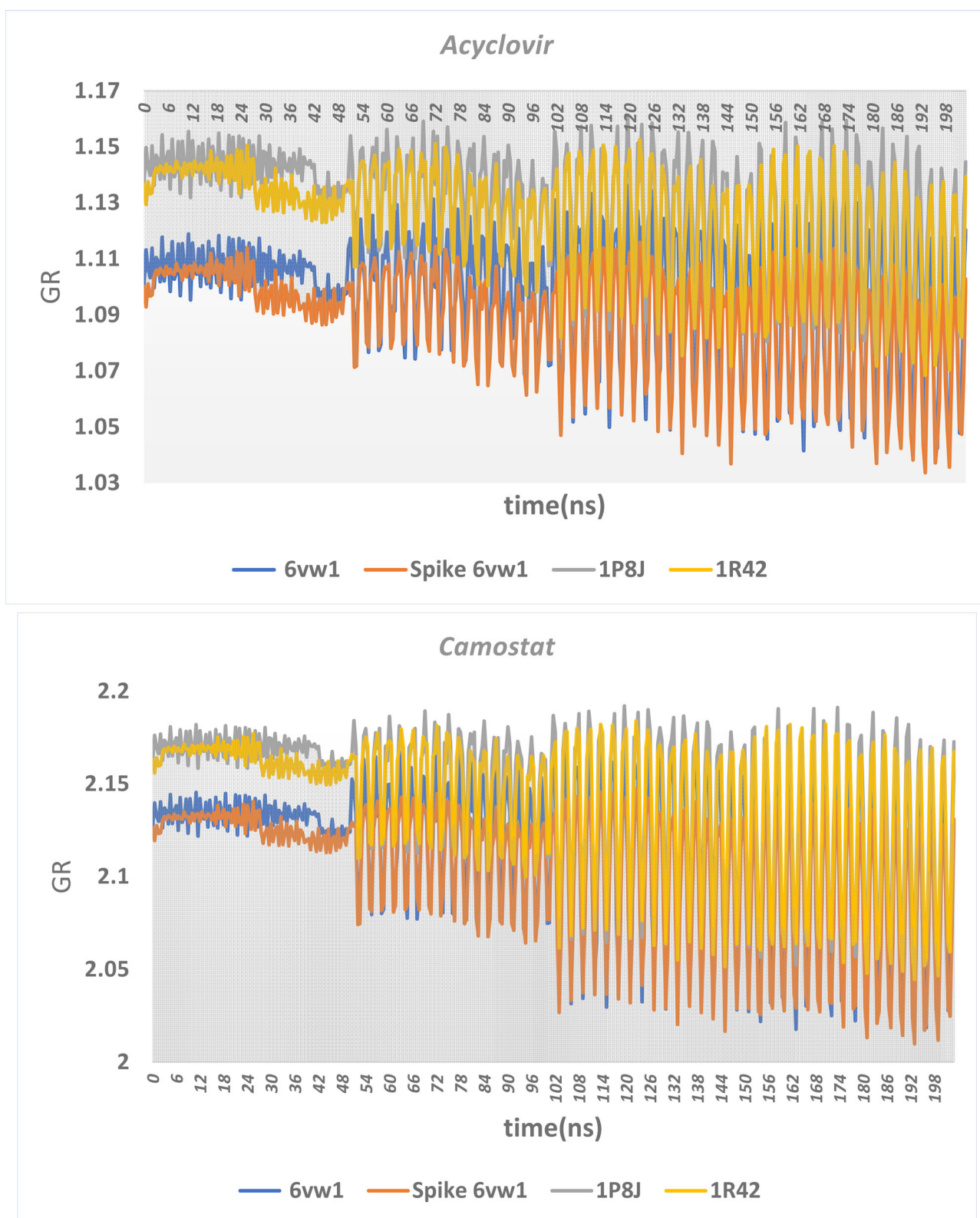
Figure 7. (Continued)

deviation for MM-GBSA BEs overall time-scale figured that strong interaction between Ligands and all examined M^Pros. The investigated compounds also examined their interactions through individual residues during MDs. The tested compounds stabilized in Spike-ACE2 interface Complex (6VW1) by two H-bonds with Arg314 (Figure 3 & S7) before the beginning of the production step the bond still stable during

all simulations. Similarly, for ACE-2 receptor (1R42) these ligands formed stable two H-bonds with Glu208 and Arg219 during all periods of the simulation process (Figure S8). In the case of the Spike chain in the ACE-2 complex (6VW1), four stable H-bond formed with Asn375, Asn440, Asn370 and Val3.76 with bond length 2.68, 2.77, 2.66 and 2.47, respectively. The investigated ligand stabilized in Furin Protein
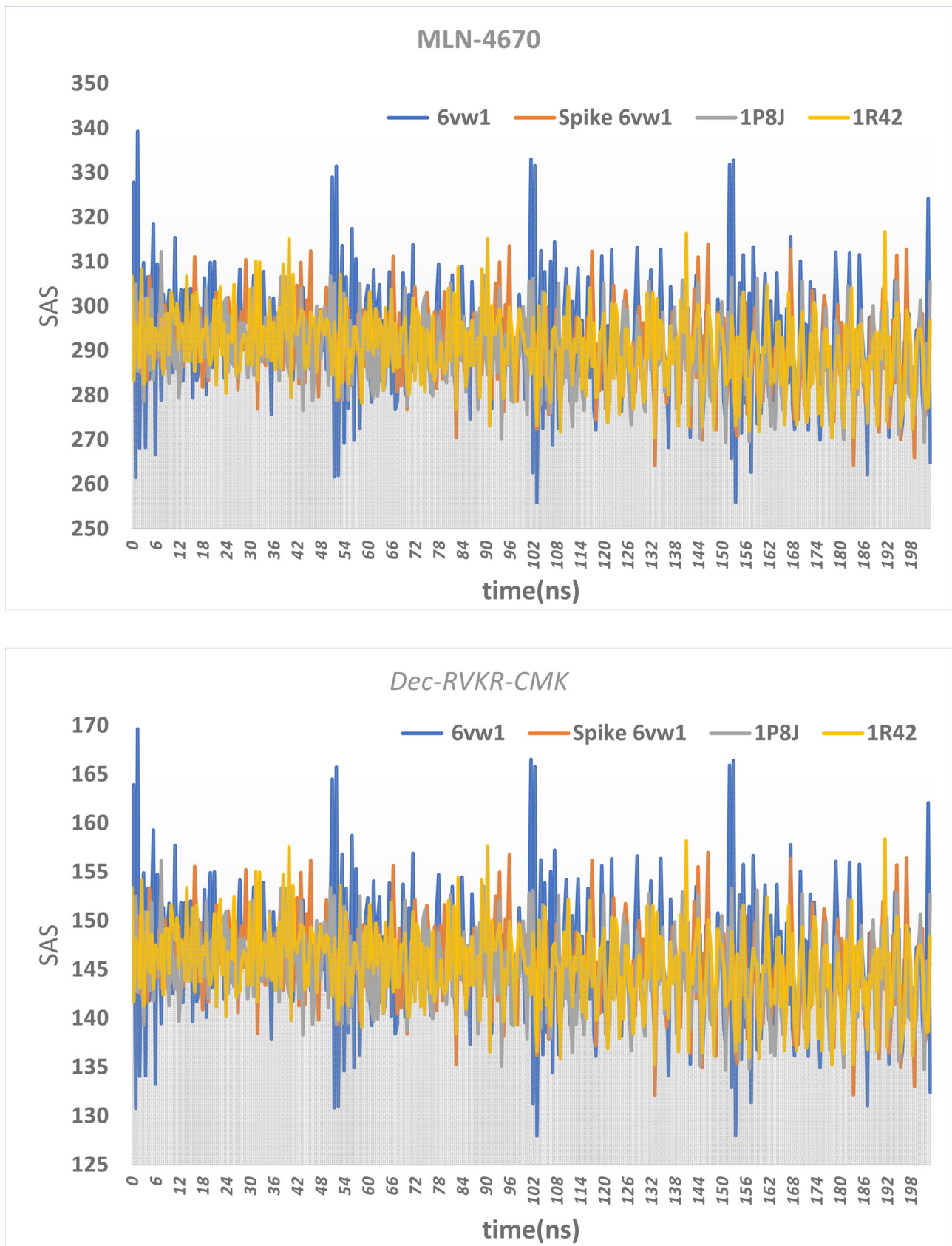
Figure 8. SASA analysis for 6vwl-Complexes (Blue), spike 6vwl-Complexes (Red), 1P8J-Complexes (gray) and 1R42-Complexe (yellow).

(1PJ8) by forming three H-bond Ala532 and Lys449 during all 50 ns (Figures 3, 4 and S7). The super-position of ligands conformation between the starting and end of MDs figured the stability of the complex. The equilibrated RMSD ligand confirms this data during all the simulation process (Figures 3, 4, S7, and S8).
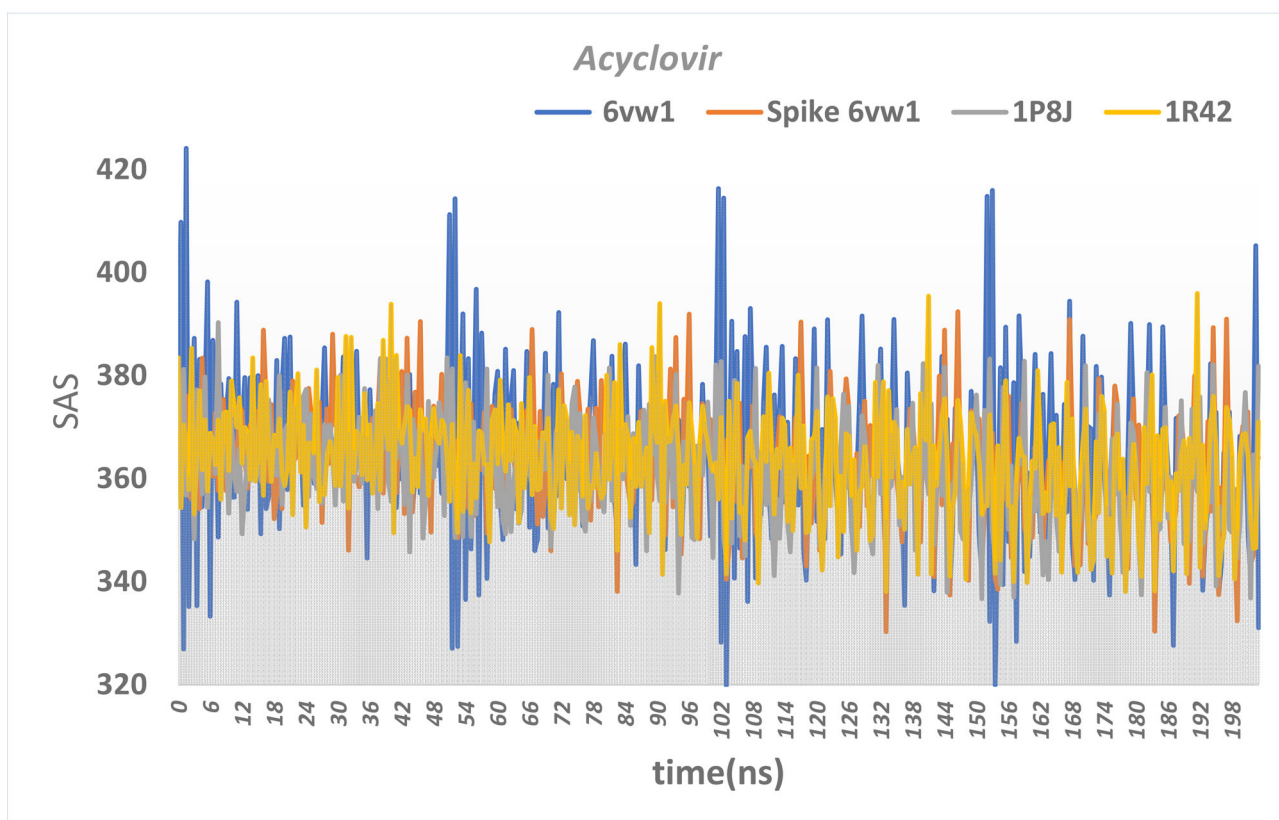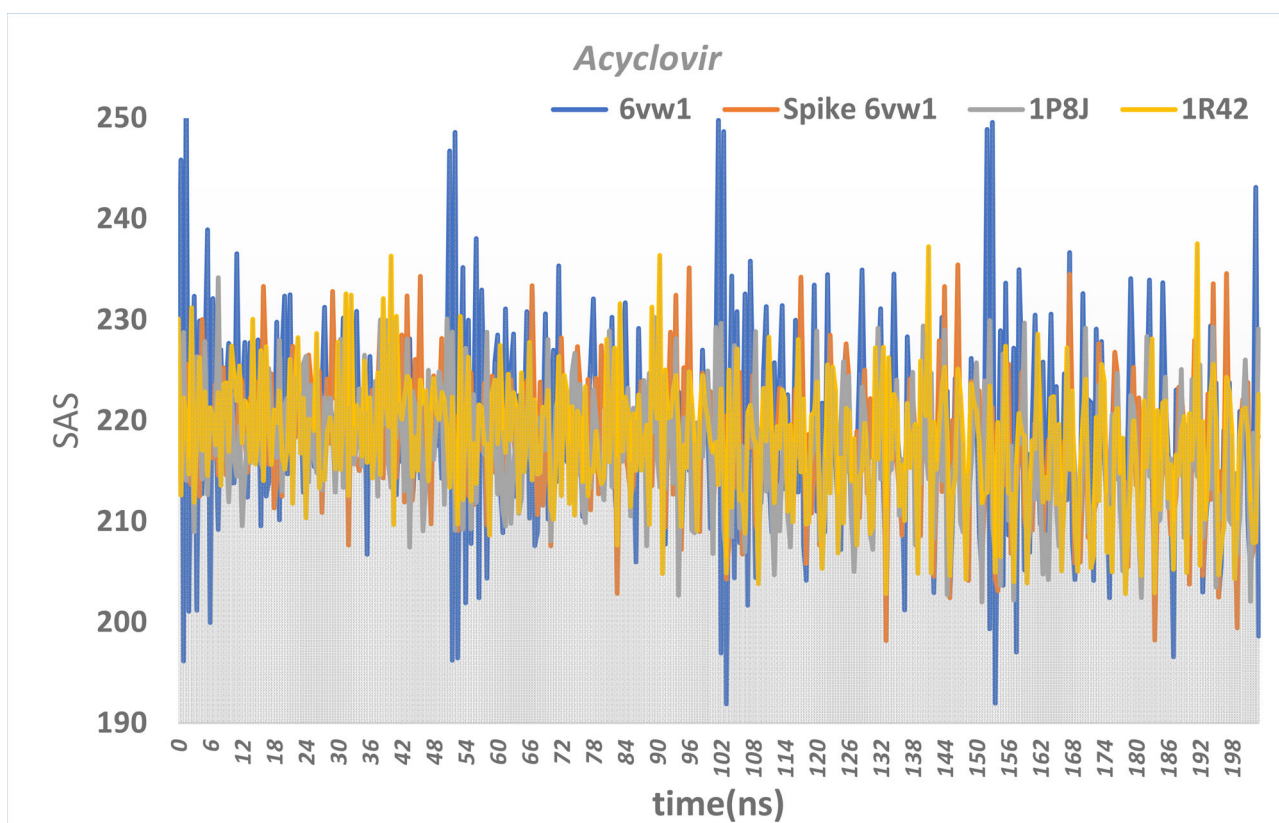
Figure 8. (Continued)

3.4. H-Bond analysis

The H-bond played an important role in identifying the stability of the interaction-strength in ligand and protein. The

MLN-4670-M^{Pro} and Dec-RVKR-CMK-M^{Pro} have constant H-bonds range between 3 and 10 in the simulation process. While Camostat-M^{Pro} and Acyclovir-M^{Pro} showed the H-interaction between 2 and 10. The changing H-bond between

ligand-M^{Pros} may propose that the conformational around ligands inside the binding site change through simulation. Overall simulations supported the high stability of all protein-ligand complexes during a simulation.

3.5. Radius-gyration (Rg) profile

The Rg was simulated to investigate the quality of the folding-system of protein with the time. The higher Rg values indicated a lower-unfolded structure combined with Harmonic-entropy. The decrease in Rg values describes the strong folded with high stability for the M^{Pro}. As it seems from (Figure 7), the Rg simulation values for MLN-4670-M^{Pros} (1.04–1.12 nm), RVKR-CMK-M^{Pros} (1.04–1.12 nm), Camostat-M^{Pros} (1.09–1.16) and Acyclovir-M^{Pros} (2.11–2.18 nm) against four cases of proteins. The difference between initial and final values for Rg simulations arranged as Camostat-M^{Pro} (0.2 nm) $<$ Acyclovir-M^{Pro} (0.14 nm) $<$ Dec-RVKR-CMK-M^{Pro} (0.1 nm) $<$ MLN-4670-M^{Pro} (0.08 nm).The lower deviation in the Rg value displayed protein's stability in the binding process and did not motivate changes in the architecture structure. These Rg values of all M^{Pros}-ligand complexes support their folded conformation structure and size.

3.6. SASA profile

The SASA (solvent accessible surface area) calculations were used for the examination of exposed receptors to solvents through MD (Figure 8) (Chaudhary et al., 2020). The binding hydrophobic-residues with ligand and exposed to solvents in the receptor affect the SASA values. The SASA value exhibited between 130–420 nm^2, which displayed that ligands' binding does not change in the folding conformation of the protein.

4. Conclusion

SARS-Cov-2 was believed to be a pandemic virus, and it thought that blocking viral spike protein and/or ACE-2 receptors could help in improving a drug or vaccines against Covid-19, that is why the present work focused on small molecules which had the abilities to work against SARS-Cov-2 through disrupting the spike-ACE-2 interaction. The small molecules used in this study were EDTA disodium salt, MLN-4670, DEC-RVKR-CMK, Acyclovir, and Camostat. The current study by docking studies revealed that the most bindings showed to Spike-ACE-2 interface complex, ACE-2 receptor, Spike protein and Furin were EDTA, MLN-4670 and DEC-RVKR-CML. Further, the 200 ns MDs confirmed the affinity for investigated molecules from lower calculated MM-GBSA, RMSD deviations and better stabilization in spike receptor-binding domain of M^{Pros}. This study highlighted small molecules that could act as potential therapeutic drugs against Covid-19; this purpose requires practical experiments as a clinical trial research in-vitro and in-vivo studies.

ORCID

Essam S. A. E. H. Khattab http://orcid.org/0000-0003-1863-9198
Ahmed Ragab http://orcid.org/0000-0001-8542-7465
Mahmoud A. Abol-Ftouh http://orcid.org/0000-0002-0506-8667
Ahmed A. Elhenawy http://orcid.org/0000-0003-2893-0376

Reference

Ammar, Y. A., Abbas, S. Y., El-Sharief, M. A. M. S., Salem, M. A. E.-R., & Mohamed, A. R. (2017). Synthesis and characterization of new imidazolidineiminothione and bis-imidazolidineiminothione derivatives as potential antimicrobial agents. European Journal of Chemistry, 8(1), 76–81. https://doi.org/10.5155/eurjchem.8.1.76-81.1542

Ammar, Y. A., El-Hafez, S. M. A. A., Hessein, S. A., Ali, A. M., Askar, A. A., & Ragab, A. (2021). One-pot strategy for thiazole tethered 7-ethoxy quinoline hybrids: Synthesis and potential antimicrobial agents as dihydrofolate reductase (DHFR) inhibitors with molecular docking study. Journal of Molecular Structure, 1242, 130748. https://doi.org/10.1016/j.molstruc.2021.130748

Ammar, Y. A., El-Sharief, M. A. M. S., Ghorab, M. M., Mohamed, Y. A., Ragab, A., & Abbas, S. Y. (2016). New imidazolidineiminothione, imidazolidin-2-one and imidazoquinoxaline derivatives: Synthesis and evaluation of antibacterial and antifungal activities. Current Organic Synthesis, 13(3), 466–475. https://doi.org/10.2174/1570179412666150817221755

Ammar, Y. A., Farag, A. A., Ali, A. M., Hessein, S. A., Askar, A. A., Fayed, E. A., Elsisi, D. M., & Ragab, A. (2020a). Antimicrobial evaluation of thiadiazino and thiazolo quinoxaline hybrids as potential DNA gyrase inhibitors; design, synthesis, characterization and morphological studies. Bioorganic Chemistry, 99, 103841. https://doi.org/10.1016/j.bioorg.2020.103841

Ammar, Y. A., Farag, A. A., Ali, A. M., Ragab, A., Askar, A. A., Elsisi, D. M., & Belal, A. (2020b). Design, synthesis, antimicrobial activity and molecular docking studies of some novel di-substituted sulfonylquinoxaline derivatives. Bioorganic Chemistry, 104, 104164. https://doi.org/10.1016/j.bioorg.2020.104164

Ammar, Y. A., Sh El-Sharief, A. M., Belal, A., Abbas, S. Y., Mohamed, Y. A., Mehany, A. B. M., & Ragab, A. (2018). Design, synthesis, antiproliferative activity, molecular docking and cell cycle analysis of some novel (morpholinosulfonyl) isatins with potential EGFR inhibitory activity. European Journal of Medicinal Chemistry, 156, 918–932. https://doi.org/10.1016/j.ejmech.2018.06.061

Baron, S. A., Devaux, C., Colson, P., Raoult, D., & Rolain, J.-M. (2020). Teicoplanin: An alternative drug for the treatment of COVID-19? International Journal of Antimicrobial Agents, 55(4), 105944. https://doi.org/10.1016/j.ijantimicag.2020.105944

Becker, G. L., Sielaff, F., Than, M. E., Lindberg, I., Routhier, S., Day, R., Lu, Y., Garten, W., & Steinmetzer, T. (2010). Potent inhibitors of Furin and Furin-like proprotein convertases containing decarboxylated P1 arginine mimetics. *Journal of Medicinal Chemistry*, 53(3), 1067–1075. https://doi.org/10.1021/jm9012455

Benson, N. C., & Daggett, V. (2012). A comparison of multiscale methods for the analysis of molecular dynamics simulations. *The Journal of Physical Chemistry B*, 116(29), 8722–8731. https://doi.org/10.1021/jp302103t

Chappel, M. C., & Ferrario, C. M. (2006). ACE and ACE2: Their role to balance the expression of angiotensin II and angiotensin-(1-7)). *Kidney International*, 70(1), 8–10. https://doi.org/10.1038/sj.ki.5000321

Chaudhary, M., Kumar, N., Baldi, A., Chandra, R., Babu, M. A., & Madan, J. (2020). 4-Bromo-4′-chloro pyrazoline analog of curcumin augmented anticancer activity against human cervical cancer, HeLa cells: in silico-guided analysis, synthesis, and in vitro cytotoxicity. *Journal of Biomolecular Structure & Dynamics*, 38(5), 1335–1353. https://doi.org/10.1080/07391102.2019.1604266

Coutard, B., Valle, C., de Lamballerie, X., Canard, B., Seidah, N. G., & Decroly, E. (2020). The spike glycoprotein of the new coronavirus 2019-nCoV contains a furin-like cleavage site absent in CoV of the same clade. *Antiviral Research*, 176, 104742. https://doi.org/10.1016/j.antiviral.2020.104742

Day, P. M., & Schiller, J. T. (2009). The role of furin in papillomavirus infection. *Future Microbiol*, 4(10), 1255–1262. https://doi.org/10.2217/fmb.09.86

de Wit, E., van Doremalen, N., Falzarano, D., & Munster, V. J. (2016). SARS and MERS: Recent insights into emerging coronaviruses. *Nature Reviews. Microbiology*, 14(8), 523–534. https://doi.org/10.1038/nrmicro.2016.81

Devaux, C. A., Rolain, J.-M., Colson, P., & Raoult, D. (2020). New insights on the antiviral effects of chloroquine against coronavirus: What to expect for COVID-19? *International Journal of Antimicrobial Agents*, 55(5), 105938. https://doi.org/10.1016/j.ijantimicag.2020.105938

Durmaz, B., Abdulmajed, O., & Durmaz, R. (2020). Mutations observed in the SARS-CoV-2 spike glycoprotein and their effects in the interaction of virus with ACE-2 receptor. *Medeniyet Medical Journal*, 35(3), 253–260. https://doi.org/10.5222/MMJ.2020.98048

El-Houseini, M. E., Refaei, M. O., Amin, A. I., & Abol-Ftouh, M. A. (2013). Potential role of curcumin and taurine combination therapy on human myeloid leukemic cells propagated in vitro. *Leukemia & Lymphoma*, 54(10), 2281–2287. https://doi.org/10.3109/10428194.2013.776167

El-Sharief, A. M. S., Ammar, Y. A., Belal, A., El-Sharief, M. A. M. S., Mohamed, Y. A., Mehany, A. B. M., Elhag Ali, G. A. M., & Ragab, A. (2019). Design, synthesis, molecular docking and biological activity evaluation of some novel indole derivatives as potent anticancer active agents and apoptosis inducers. *Bioorganic Chemistry*, 85, 399–412. https://doi.org/10.1016/j.bioorg.2019.01.016

El-Sharief, M. A. M. S., Abbas, S. Y., Zahran, M. A., Mohamed, Y. A., Ragab, A., & Ammar, Y. A. (2016). New 1,3-diaryl-5-thioxo-imidazolidin-2,4-dione derivatives: Synthesis, reactions and evaluation of antibacterial and antifungal activities. *Zeitschrift Für Naturforschung B*, 71(8), 875–881. https://doi.org/10.1515/znb-2016-0054

El-Shimy, I. A., Mohamed, M. M. A., Hasan, S. S., & Hadi, M. A. (2021). Targeting host cell proteases as a potential treatment strategy to limit the spread of SARS-CoV-2 in the respiratory tract. *Pharmacology Research & Perspectives*, 9(1), e00698. https://doi.org/10.1002/prp2.698

Fayed, E. A., Ammar, Y. A., Ragab, A., Gohar, N. A., Mehany, A. B. M., & Farrag, A. M. (2020). In vitro cytotoxic activity of thiazole-indenoquinoxaline hybrids as apoptotic agents, design, synthesis, physicochemical and pharmacokinetic studies. *Bioorganic Chemistry*, 100, 103951. https://doi.org/10.1016/j.bioorg.2020.103951

Fukuda, T., Umeki, T., Tokushima, K., Xiang, G., Yoshida, Y., Ishibashi, F., Oku, Y., Nishiya, N., Uehara, Y., & Iwao, M. (2017). Design, synthesis, and evaluation of A-ring-modified lamellarin N analogues as noncovalent inhibitors of the EGFR T790M/L858R mutant. *Bioorganic & Medicinal Chemistry*, 25(24), 6563–6580. https://doi.org/10.1016/j.bmc.2017.10.030

Fulgenzi, A., & Ferrero, E. M. (2019). EDTA chelation therapy for the treatment of neurotoxicity. *International Journal of Molecular Sciences*, 20(5), 1019. https://doi.org/10.3390/ijms20051019

Gajula, M. N. V. P. P., Kumar, A., & Ijaq, J. (2016). Protocol for molecular dynamics simulations of proteins. *Bio-Protocol*, 6(23), e2051. https://doi.org/10.21769/BioProtoc.2051

Garten, W., Hallenberger, S., Ortmann, D., Schäfer, W., Vey, M., Angliker, H., Shaw, E., & Klenk, H. D. (1994). Processing of viral glycoproteins by the subtilisin-like endoprotease furin and its inhibition by specific peptidylchloroalkylketones. *Biochimie*, 76(3–4), 217–225. https://doi.org/10.1016/0300-9084(94)90149-X

Gordon, J. C., Myers, J. B., Folta, T., Shoja, V., Heath, L. S., & Onufriev, A. (2005). H++: A server for estimating pKas and adding missing hydrogens to macromolecules. *Nucleic Acids Research*, 33(Web Server issue), W368–W371. https://doi.org/10.1093/nar/gki464

Grier, M. T., & Meyers, D. G. (1993). So much writing, so little science: A review of 37 years of literature on edetate sodium chelation therapy. *The Annals of Pharmacotherapy*, 27(12), 1504–1509. https://doi.org/10.1177/106002809302701217

Halbert, S. C. (2004). Chelation therapy for cardiovascular disease BT. In R. A. Stein, M. C. Oz (Eds.), *Complementary and alternative cardiovascular medicine* (pp. 189–200). Humana Press. https://doi.org/10.1007/978-1-59259-728-4_12

Hallenberger, S., Bosch, V., Angliker, H., Shaw, E., Klenk, H.-D., & Garten, W. (1992). Inhibition of furin-mediated cleavage activation of HIV-1 glycoprotein gp160. *Nature*, 360(6402), 358–361. https://doi.org/10.1038/360358a0

Hassan, A. S., Askar, A. A., Naglah, A. M., Almehizia, A. A., & Ragab, A. (2020). Discovery of new Schiff bases tethered pyrazole moiety: design, synthesis, biological evaluation, and molecular docking study as dual targeting DHFR/DNA gyrase inhibitors with immunomodulatory activity. *Molecules*, 25(11), 2593. https://doi.org/10.3390/molecules25112593

Hassan, A. S., Morsy, N. M., Awad, H. M., & Ragab, A. (2021). Synthesis, molecular docking, and in silico ADME prediction of some fused pyrazolo[1,5-a]pyrimidine and pyrazole derivatives as potential antimicrobial agents. *Journal of the Iranian Chemical Society*. https://doi.org/10.1007/s13738-021-02319-4

Heald-Sargent, T., & Gallagher, T. (2012). Ready, set, fuse! The coronavirus spike protein and acquisition of fusion competence. *Viruses*, 4(4), 557–580. https://doi.org/10.3390/v4040557

Henrich, S., Cameron, A., Bourenkov, G. P., Kiefersauer, R., Huber, R., Lindberg, I., Bode, W., & Than, M. E. (2003). The crystal structure of the proprotein processing proteinase furin explains its stringent specificity. *Nature Structural Biology*, 10(7), 520–526. https://doi.org/10.1038/nsb941

Hoffmann, M., Kleine-Weber, H., Schroeder, S., Krüger, N., Herrler, T., Erichsen, S., Schiergens, T. S., Herrler, G., Wu, N.-H., Nitsche, A., Müller, M. A., Drosten, C., & Pöhlmann, S. (2020). SARS-CoV-2 cell entry depends on ACE2 and TMPRSS2 and is blocked by a clinically proven protease inhibitor. *Cell*, 181(2), 271–280.e8. https://doi.org/10.1016/j.cell.2020.02.052

Ibrahim, S. A., Fayed, E. A., Rizk, H. F., Desouky, S. E., & Ragab, A. (2021a). Hydrazonoyl bromide precursors as DHFR inhibitors for the synthesis of bis-thiazolyl pyrazole derivatives; antimicrobial activities, antibiofilm, and drug combination studies against MRSA. *Bioorganic Chemistry*, 116, 105339. https://doi.org/10.1016/j.bioorg.2021.105339

Ibrahim, S. A., Rizk, H. F., Aboul-Magd, D. S., & Ragab, A. (2021b). Design, synthesis of new magenta dyestuffs based on thiazole azomethine disperse reactive dyes with antibacterial potential on both dyes and gamma-irradiated dyed fabric. *Dyes and Pigments*, 193, 109504. https://doi.org/10.1016/j.dyepig.2021.109504

Kong, R., Yang, G., Xue, R., Liu, M., Wang, F., Hu, J., Guo, X., & Chang, S. (2020). COVID-19 Docking Server: An interactive server for docking small molecules, peptides and antibodies against potential targets of COVID-19. *arXiv Prepr*. arXiv2003.00163.

Lai, C.-C., Liu, Y. H., Wang, C.-Y., Wang, Y.-H., Hsueh, S.-C., Yen, M.-Y., Ko, W.-C., & Hsueh, P.-R. (2020). Asymptomatic carrier state, acute respiratory disease, and pneumonia due to severe acute respiratory syndrome coronavirus 2 (SARS-CoV-2): Facts and myths. *Journal of*

Microbiology, Immunology, and Infection = Wei Mian yu Gan Ran za Zhi, 53(3), 404–412. https://doi.org/10.1016/j.jmii.2020.02.012

Lamas, G. A., Goertz, C., Boineau, R., Mark, D. B., Rozema, T., Nahin, R. L., Lindblad, L., Lewis, E. F., Drisko, J., Lee, K. L., & TACT Investigators. (2013). Effect of disodium EDTA chelation regimen on cardiovascular events in patients with previous myocardial infarction: The TACT randomized trial. *JAMA*, 309(12), 1241–1250. https://doi.org/10.1001/jama.2013.2107

Li, W., Moore, M. J., Vasilieva, N., Sui, J., Wong, S. K., Berne, M. A., Somasundaran, M., Sullivan, J. L., Luzuriaga, K., Greenough, T. C., Choe, H., & Farzan, M. (2003). Angiotensin-converting enzyme 2 is a functional receptor for the SARS coronavirus. *Nature*, 426(6965), 450–454. https://doi.org/10.1038/nature02145

Lillie, P. J., Samson, A., Li, A., Adams, K., Capstick, R., Barlow, G. D., Easom, N., Hamilton, E., Moss, P. J., Evans, A., Ivan, M., Taha, Y., Duncan, C. J. A., & Schmid, M. L., & The Airborne HCID Network, PHE Incident Team. (2020). Novel coronavirus disease (Covid-19): The first two patients in the UK with person to person transmission. *Journal of Infection*, 80, 578–606. https://doi.org/10.1016/j.jinf.2020.02.020

Liu, C., Zhou, Q., Li, Y., Garner, L. V., Watkins, S. P., Carter, L. J., Smoot, J., Gregg, A. C., Daniels, A. D., Jervey, S., & Albaiu, D. (2020). Research and development on therapeutic agents and vaccines for COVID-19 and related human coronavirus diseases. *ACS Central Science*, 6(3), 315–331. https://doi.org/10.1021/acscentsci.0c00272

Luan, B., Huynh, T., Cheng, X., Lan, G., & Wang, H.-R. (2020). Targeting proteases for treating COVID-19. *Journal of Proteome Research*, 19(11), 4316–4326. https://doi.org/10.1021/acs.jproteome.0c00430

Madu, I. G., Roth, S. L., Belouzard, S., & Whittaker, G. R. (2009). Characterization of a highly conserved domain within the severe acute respiratory syndrome coronavirus spike protein S2 domain with characteristics of a viral fusion peptide. *Journal of Virology*, 83(15), 7411–7421. https://doi.org/10.1128/JVI.00079-09

Matsuyama, S., Shirato, K., Kawase, M., Terada, Y., Kawachi, K., Fukushi, S., & Kamitani, W. (2018). Middle east respiratory syndrome coronavirus spike protein is not activated directly by cellular furin during viral entry into target cells. *Journal of Virology*, 92, e00683–18. https://doi.org/10.1128/JVI.00683-18

Miller, A. J., & Arnold, A. C. (2019). The renin-angiotensin system in cardiovascular autonomic control: Recent developments and clinical implications. *Clinical Autonomic Research: Official Journal of the Clinical Autonomic Research Society*, 29(2), 231–243. https://doi.org/10.1007/s10286-018-0572-5

Millet, J. K., & Whittaker, G. R. (2014). Host cell entry of Middle East respiratory syndrome coronavirus after two-step, furin-mediated activation of the spike protein. *Proceedings of the National Academy of Sciences of the United States of America*, 111(42), 15214–15219. https://doi.org/10.1073/pnas.1407087111

Millet, J. K., & Whittaker, G. R. (2015). Host cell proteases: Critical determinants of coronavirus tropism and pathogenesis. *Virus Research*, 202, 120–134. https://doi.org/10.1016/j.virusres.2014.11.021

Ohkoshi, M. (1981). Inhibition of growth of 3-methylcholanthrene-induced mouse skin tumor by protease inhibitor [N,N-dimethylcarbamoylmethyl 4-(4-guanidinobenzoyloxy)-phenylacetate] methanesulfate. *Gann*, 72, 959–964.

Ozden, S., Lucas-Hourani, M., Ceccaldi, P.-E., Basak, A., Valentine, M., Benjannet, S., Hamelin, J., Jacob, Y., Mamchaoui, K., Mouly, V., Desprès, P., Gessain, A., Butler-Browne, G., Chrétien, M., Tangy, F., Vidalain, P.-O., & Seidah, N. G. (2008). Inhibition of Chikungunya virus infection in cultured human muscle cells by furin inhibitors: Impairment of the maturation of the E2 surface glycoprotein. *The Journal of Biological Chemistry*, 283(32), 21899–21908. https://doi.org/10.1074/jbc.M802444200

Pang, Y. J., Tan, X. J., Li, D. M., Zheng, Z. H., Lei, R. X., & Peng, X. M. (2013). Therapeutic potential of furin inhibitors for the chronic infection of hepatitis B virus. *Liver International : official Journal of the International Association for the Study of the Liver*, 33(8), 1230–1238. https://doi.org/10.1111/liv.12185

Papa, G., Mallery, D. L., Albecka, A., Welch, L. G., Cattin-Ortolá, J., Luptak, J., Paul, D., McMahon, H. T., Goodfellow, I. G., Carter, A., Munro, S., & James, L. C. (2021). Furin cleavage of SARS-CoV-2 spike promotes but

is not essential for infection and cell-cell fusion. *PLoS Pathogens*, 17(1), e1009246. https://doi.org/10.1371/journal.ppat.1009246

Perry, C. M., & Wagstaff, A. J. (1995). Famciclovir. A review of its pharmacological properties and therapeutic efficacy in herpesvirus infections. *Drugs*, 50(2), 396–415. https://doi.org/10.2165/00003495-199550020-00011

Ragab, A., Fouad, S. A., Ali, O. A. A., Ahmed, E. M., Ali, A. M., Askar, A. A., & Ammar, Y. A. (2021). Sulfaguanidine hybrid with some new pyridine-2-one derivatives: Design, synthesis, and antimicrobial activity against multidrug-resistant bacteria as dual DNA gyrase and DHFR inhibitors. *Antibiotics*, 10(2), 162. https://doi.org/10.3390/antibiotics10020162

RCSB Protien Data Bank. 2020. Retrieved April 5, 2020, from https://www.rcsb.org/structure/6VW1, https://www.rcsb.org/structure/1p8j; and https://www.rcsb.org/structure/1R42

Rizk, H. F., El-Borai, M. A., Ragab, A., & Ibrahim, S. A. (2020). Design, synthesis, biological evaluation and molecular docking study based on novel fused pyrazolothiazole scaffold. *Journal of the Iranian Chemical Society*, 17(10), 2493–2505. https://doi.org/10.1007/s13738-020-01944-9

Sadjadi, S.-A., Regmi, S., & Chau, T. (2018). Acyclovir neurotoxicity in a peritoneal dialysis patient: report of a case and review of the pharmacokinetics of acyclovir. *The American Journal of Case Reports*, 19, 1459–1462. https://doi.org/10.12659/AJCR.911520

Salem, M. A., Ragab, A., Askar, A. A., El-Khalafawy, A., & Makhlouf, A. H. (2020a). One-pot synthesis and molecular docking of some new spiropyranindol-2-one derivatives as immunomodulatory agents and *in vitro* antimicrobial potential with DNA gyrase inhibitor. *European Journal of Medicinal Chemistry*, 188, 111977. https://doi.org/10.1016/j.ejmech.2019.111977

Salem, M. A., Ragab, A., El-Khalafawy, A., Makhlouf, A. H., Askar, A. A., & Ammar, Y. A. (2020b). Design, synthesis, in vitro antimicrobial evaluation and molecular docking studies of indol-2-one tagged with morpholinosulfonyl moiety as DNA gyrase inhibitors. *Bioorganic Chemistry*, 96, 103619. https://doi.org/10.1016/j.bioorg.2020.103619

Shagufta, & Ahmad, I. (2021). The race to treat COVID-19: Potential therapeutic agents for the prevention and treatment of SARS-CoV-2. *European Journal of Medicinal Chemistry*, 213, 113157. https://doi.org/10.1016/j.ejmech.2021.113157

Shah, B., Modi, P., & Sagar, S. R. (2020). *In silico* studies on therapeutic agents for COVID-19: Drug repurposing approach. *Life Science*, 252, 117652. https://doi.org/10.1016/j.lfs.2020.117652

Sinha, S. K., Prasad, S. K., Islam, M. A., Gurav, S. S., Patil, R. B., AlFaris, N. A., Aldayel, T. S., AlKehayez, N. M., Wabaidur, S. M., & Shakya, A. (2020). Identification of bioactive compounds from *Glycyrrhiza glabra* as possible inhibitor of SARS-CoV-2 spike glycoprotein and non-structural protein-15: A pharmacoinformatics study. *Journal of Biomolecular Structure and Dynamics*, 39(13), 1–15. https://doi.org/10.1080/07391102.2020.1779132

Soler, M. J., Wysocki, J., Ye, M., Lloveras, J., Kanwar, Y., & Batlle, D. (2007). ACE2 inhibition worsens glomerular injury in association with increased ACE expression in streptozotocin-induced diabetic mice. *Kidney International*, 72(5), 614–623. https://doi.org/10.1038/sj.ki.5002373

Su, S., Wong, G., Shi, W., Liu, J., Lai, A. C. K., Zhou, J., Liu, W., Bi, Y., & Gao, G. F. (2016). Epidemiology, genetic recombination, and pathogenesis of coronaviruses. *Trends in Microbiology*, 24(6), 490–502. https://doi.org/10.1016/j.tim.2016.03.003

Tong, Y., Tong, S., Zhao, X., Wang, J., Jun, J., Park, J., Wands, J., & Li, J. (2010). Initiation of duck hepatitis B virus infection requires cleavage by a Furin-like protease. *Journal of Virology*, 84(9), 4569–4578. https://doi.org/10.1128/JVI.02281-09

Tortorici, M. A., & Veesler, D. (2019). Structural insights into coronavirus entry. *Advances in Virus Research*, 105, 93–116. https://doi.org/10.1016/bs.aivir.2019.08.002

Uno, Y. (2020). Camostat mesilate therapy for COVID-19. *Internal and Emergency Medicine*, 15, 1–2. https://doi.org/10.1007/s11739-020-02345-9

Van Lam van, T., Ivanova, T., Hardes, K., Heindl, M. R., Morty, R. E., Böttcher-Friebertshäuser, E., Lindberg, I., Than, M. E., Dahms, S. O., & Steinmetzer, T. (2019). Design, synthesis, and characterization of

macrocyclic inhibitors of the proprotein convertase Furin. *Chemmedchem*, *14*(6), 673–685. https://doi.org/10.1002/cmdc.201800807

Vickers, C., Hales, P., Kaushik, V., Dick, L., Gavin, J., Tang, J., Godbout, K., Parsons, T., Baronas, E., Hsieh, F., Acton, S., Patane, M., Nichols, A., & Tummino, P. (2002). Hydrolysis of biological peptides by human angiotensin-converting enzyme-related carboxypeptidase. *The Journal of Biological Chemistry*, *277*(17), 14838–14843. https://doi.org/10.1074/jbc.M200581200

Walls, A. C., Park, Y.-J., Tortorici, M. A., Wall, A., McGuire, A. T., & Veesler, D. (2020). Structure, function, and antigenicity of the SARS-CoV-2 spike glycoprotein. *Cell*, *181*(2), 281–292.e6. https://doi.org/10.1016/j.cell.2020.02.058

Wan, Y., Shang, J., Graham, R., Baric, R. S., & Li, F. (2020). Receptor recognition by the novel coronavirus from Wuhan: An analysis based on decade-long structural studies of SARS coronavirus. *Journal of Virology*, *94*, e00127–20. https://doi.org/10.1128/JVI.00127-20

Wassel, M. M. S., Ammar, Y. A., Elhag Ali, G. A. M., Belal, A., Mehany, A. B. M., & Ragab, A. (2021a). Development of adamantane scaffold containing 1,3,4-thiadiazole derivatives: Design, synthesis, anti-proliferative activity and molecular docking study targeting EGFR. *Bioorganic Chemistry*, *110*, 104794. https://doi.org/10.1016/j.bioorg.2021.104794

Wassel, M. M. S., Ragab, A., Elhag Ali, G. A. M., Mehany, A. B. M., & Ammar, Y. A. (2021b). Novel adamantane-pyrazole and hydrazone hybridized: Design, synthesis, cytotoxic evaluation, SAR study and molecular docking simulation as carbonic anhydrase inhibitors. *Journal of Molecular Structure.*, *1223*, 128966. https://doi.org/10.1016/j.molstruc.2020.128966

Wong, S. K., Li, W., Moore, M. J., Choe, H., & Farzan, M. (2004). A 193-amino acid fragment of the SARS coronavirus S protein efficiently binds angiotensin-converting enzyme 2. *Journal of Biological Chemistry*, *279*(5), 3197–3201. https://doi.org/10.1074/jbc.C300520200

Wrapp, D., Wang, N., Corbett, K. S., Goldsmith, J. A., Hsieh, C.-L., Abiona, O., Graham, B. S., & McLellan, J. S. (2020). Cryo-EM structure of the 2019-nCoV spike in the prefusion conformation. *Science (New York, N.Y.)*, *367*(6483), 1260–1263. https://doi.org/10.1126/science.abb2507

Wu, J. T., Leung, K., & Leung, G. M. (2020). Nowcasting and forecasting the potential domestic and international spread of the 2019-nCoV outbreak originating in Wuhan, China: A modelling study. *Lancet (London, England)*, *395*(10225), 689–697. https://doi.org/10.1016/S0140-6736(20)30260-9

Wysocki, J., Ye, M., Soler, M. J., Gurley, S. B., Xiao, H. D., Bernstein, K. E., Coffman, T. M., Chen, S., & Batlle, D. (2006). ACE and ACE2 activity in diabetic mice. *Diabetes*, *55*(7), 2132–2139. https://doi.org/10.2337/db06-0033

Yamada, Y., & Liu, D. X. (2009). Proteolytic activation of the spike protein at a novel RRRR/S Motif is implicated in furin-dependent entry, syncytium formation, and infectivity of coronavirus infectious bronchitis virus in cultured cells. *Journal of Virology*, *83*(17), 8744–8758. https://doi.org/10.1128/JVI.00613-09

Ye, M., Wysocki, J., William, J., Soler, M. J., Cokic, I., & Batlle, D. (2006). Glomerular localization and expression of angiotensin-converting enzyme 2 and angiotensin-converting enzyme: Implications for albuminuria in diabetes. *Journal of the American Society of Nephrology*, *17*(11), 3067–3075. https://doi.org/10.1681/ASN.2006050423

Yepes-Pérez, A. F., Herrera-Calderon, O., & Quintero-Saumeth, J. (2020). Uncaria tomentosa (cat's claw): A promising herbal medicine against SARS-CoV-2/ACE-2 junction and SARS-CoV-2 spike protein based on molecular modeling. *Journal of Biomolecular Structure and Dynamics*, *38*, 1–17. https://doi.org/10.1080/07391102.2020.1837676

Zahoor, I., Cerghet, M., & Giri, S. (2021). Neuropathogenesis of SARS-CoV-2 Infection. Chapter 2. In A. R. Ramadan & G. B. T. Osman (Eds.), *Neurological care and the COVID-19 pandemic* (pp. 25–43). Elsevier. https://doi.org/10.1016/B978-0-323-82691-4.00006-6

Zhang, H., Penninger, J. M., Li, Y., Zhong, N., & Slutsky, A. S. (2020). Angiotensin-converting enzyme 2 (ACE2) as a SARS-CoV-2 receptor: Molecular mechanisms and potential therapeutic target. *Intensive Care Medicine*, *46*(4), 586–590. https://doi.org/10.1007/s00134-020-05985-9

Zhao, Y., Zhao, Z., Wang, Y., Zhou, Y., Ma, Y., & Zuo, W. (2020). Single-cell RNA expression profiling of ACE2, the receptor of SARS-CoV-2. *American Journal of Respiratory and Critical Care Medicine*, *202*(5), 756–759. https://doi.org/10.1164/rccm.202001-0179LE

Zhou, P., Yang, X.-L., Wang, X.-G., Hu, B., Zhang, L., Zhang, W., Si, H.-R., Zhu, Y., Li, B., Huang, C.-L., Chen, H.-D., Chen, J., Luo, Y., Guo, H., Jiang, R.-D., Liu, M.-Q., Chen, Y., Shen, X.-R., Wang, X., … Shi, Z.-L. (2020). A pneumonia outbreak associated with a new coronavirus of probable bat origin. *Nature*, *579*(7798), 270–273. https://doi.org/10.1038/s41586-020-2012-7